Science Advances
AAAS

Supplementary Materials for

Cell response to extracellular matrix viscous energy dissipation outweighs high-rigidity sensing

Carla Huerta-López *et al.*

Corresponding author: Jorge Alegre-Cebollada, jalegre@cnic.es

Sci. Adv. **10**, eadf9758 (2024)
DOI: 10.1126/sciadv.adf9758

The PDF file includes:

Figs. S1 to S19
Tables S1 to S3
Supplementary Notes S1 to S5
Legend for file S1
References

Other Supplementary Material for this manuscript includes the following:

File S1

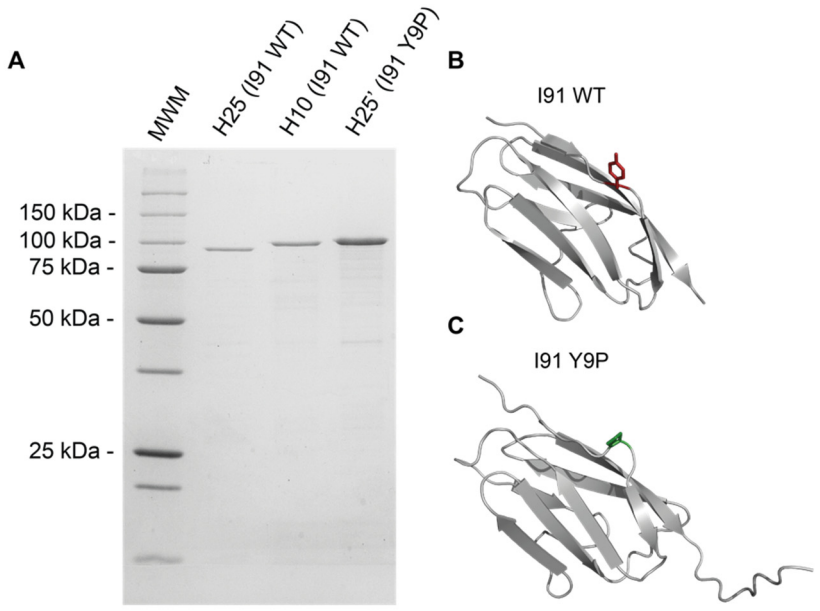

Figure S1: I91 polyprotein building blocks. (A) 12 % SDS-PAGE analysis of representative purified soluble polyproteins used in this report. MWM: Precision Plus Protein Unstained Standards (Bio-Rad). **(B)** Three-dimensional structure of monomeric I91 (PDB: 1TIT [77]). The tyrosine residue employed to crosslink proteins is highlighted in red. **(C)** Three-dimensional structure of titin I91 Y9P domain (PDB: 2RQ8 [78]). Pro9 is shown in green.

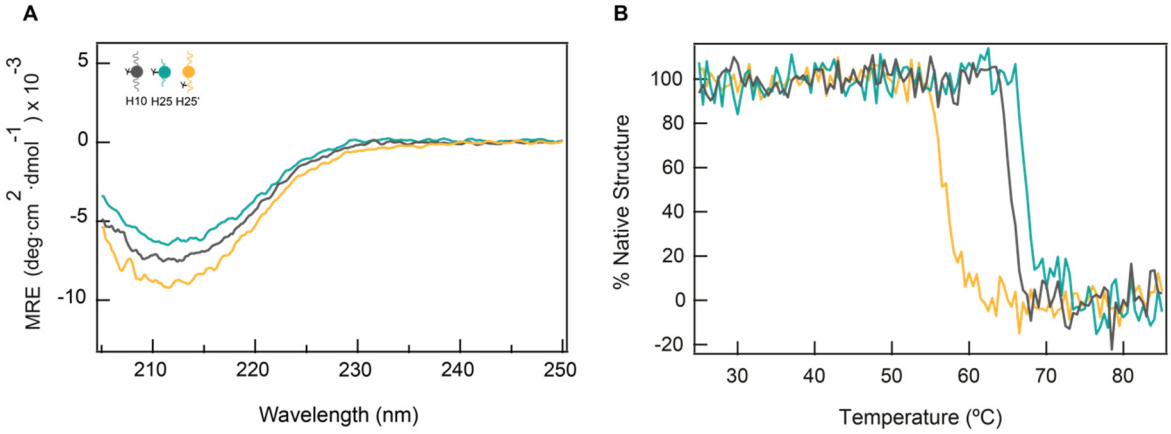

Figure S2: Thermal stability of protein building blocks by CD spectroscopy. (A) CD spectra (given as mean residue ellipticity, MRE) obtained for H10 (grey), H25 (teal) and H25' (mustard) building blocks recorded from 205 to 250 nm at 25 °C. Spectra show a minimum at ~212 nm, typical of the β–rich structure of the I91 domain [77]. **(B)** Thermal denaturation curves obtained by tracking the CD signal at 215 nm.

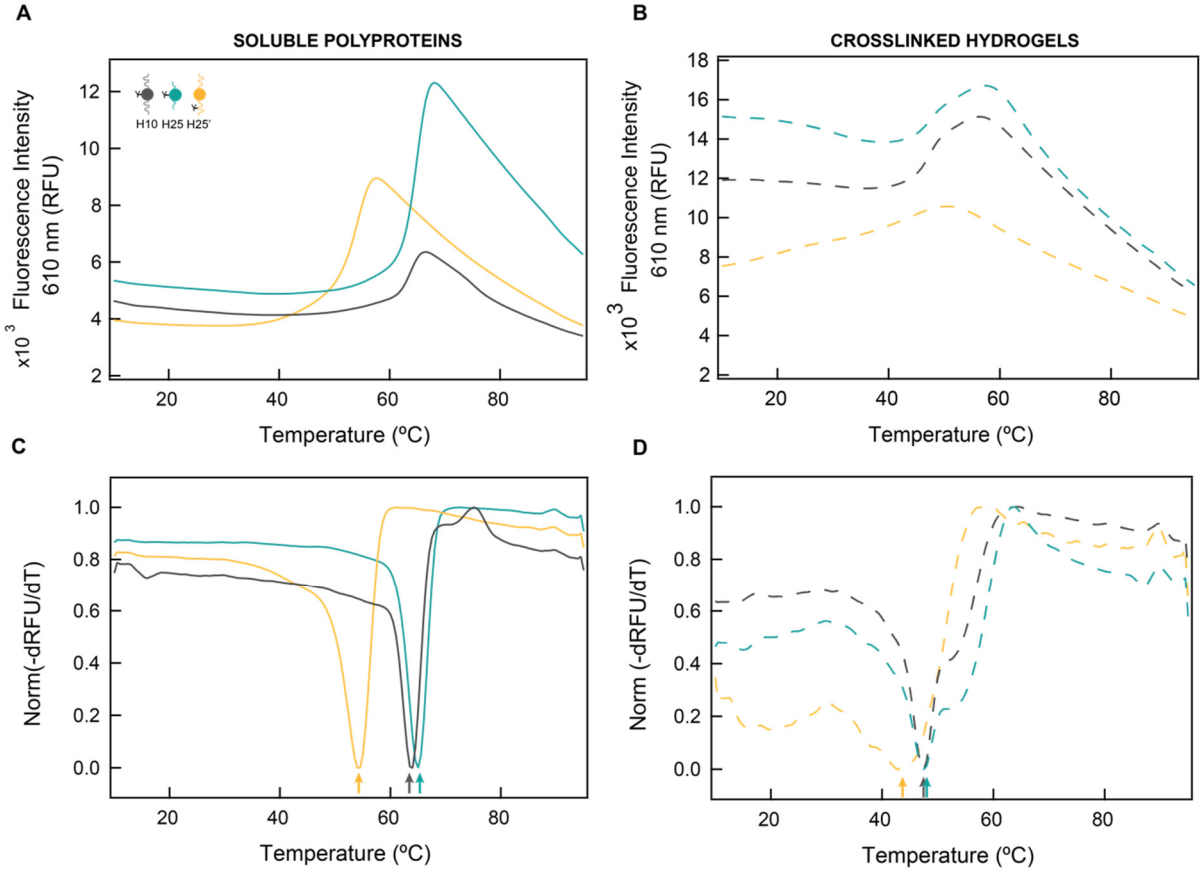

Figure S3: Polyprotein thermal stability by differential scanning fluorimetry. (A, B) Recording of fluorescence intensity versus temperature for the unfolding of soluble (A) protein building blocks, and (B) protein hydrogels. **(C, D)** First derivative fluorescent signal of (C) protein building blocks and (D) protein hydrogels. Melting temperatures are indicated by arrows.

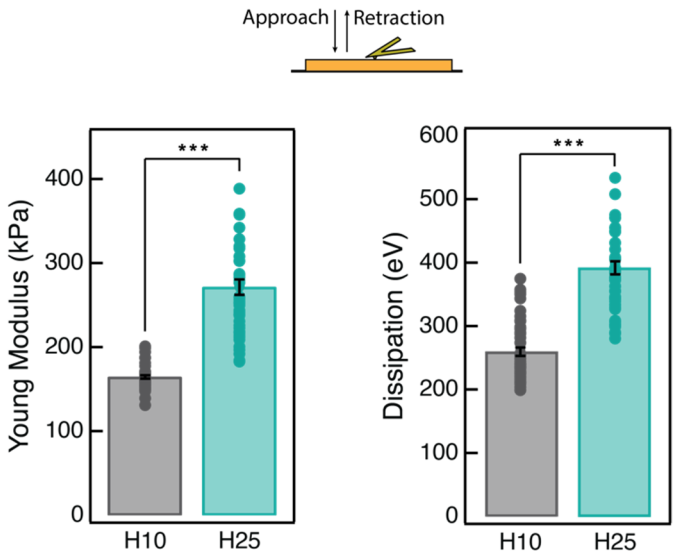

Figure S4: AFM analysis of the nanomechanics of I91-based hydrogels. Hydrogels were assayed at 10 µm/s. Specimens were characterized after being incubated at 37 ºC for 12 hours. (N = 10 indentations on 5 positions for one gel, mean ± S.E.M., unpaired two-tailed t-test, ***$p < 0.001$).

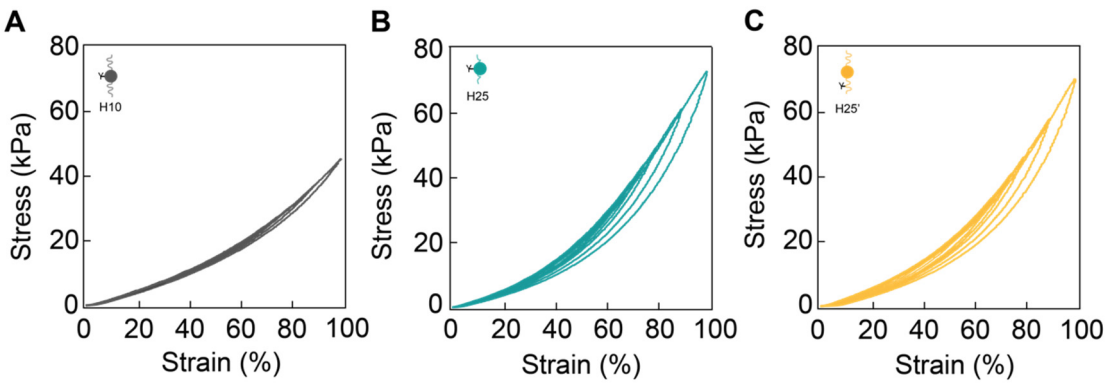

Figure S5: Tensile testing of I91 hydrogels. Representative stress-strain curves of H10 **(A)**, H25 **(B)** and H25' **(C)** hydrogels loaded and unloaded at 5 mm/s. Curves were measured immediately one after another from low to high strains. These curves are also represented in **Fig. 1E,F** with an offset in the x-axis.

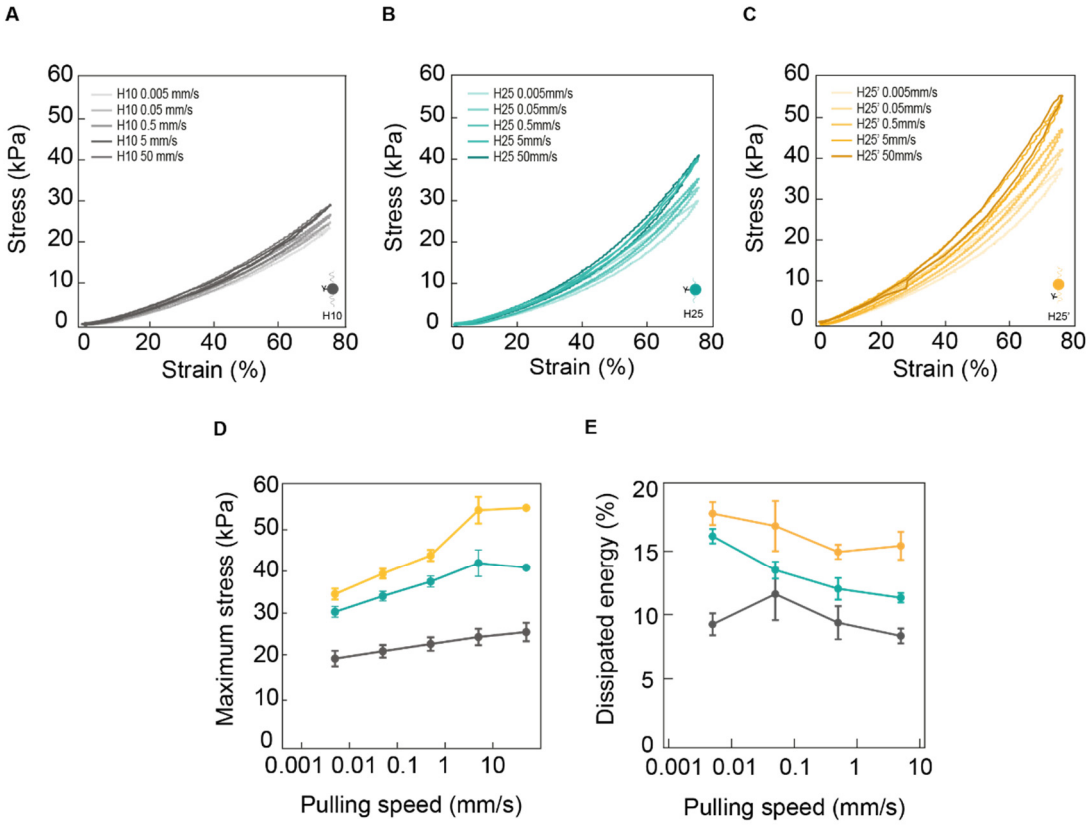

Figure S6. Mechanical behavior of I91 hydrogels under different pulling rates. (**A-C**) Stress-strain curves at 75% final strain obtained at 0.005-50 mm/s pulling speeds for materials H10 (A), H25 (B) and H25' (C). **(D)** Maximum stress at the different pulling speeds. **(E)** Dissipated energy at the different pulling speeds. Values at 50 mm/s could not be measured accurately due to instrumental limitations. Data obtained with 3 specimens from a single protein purification.

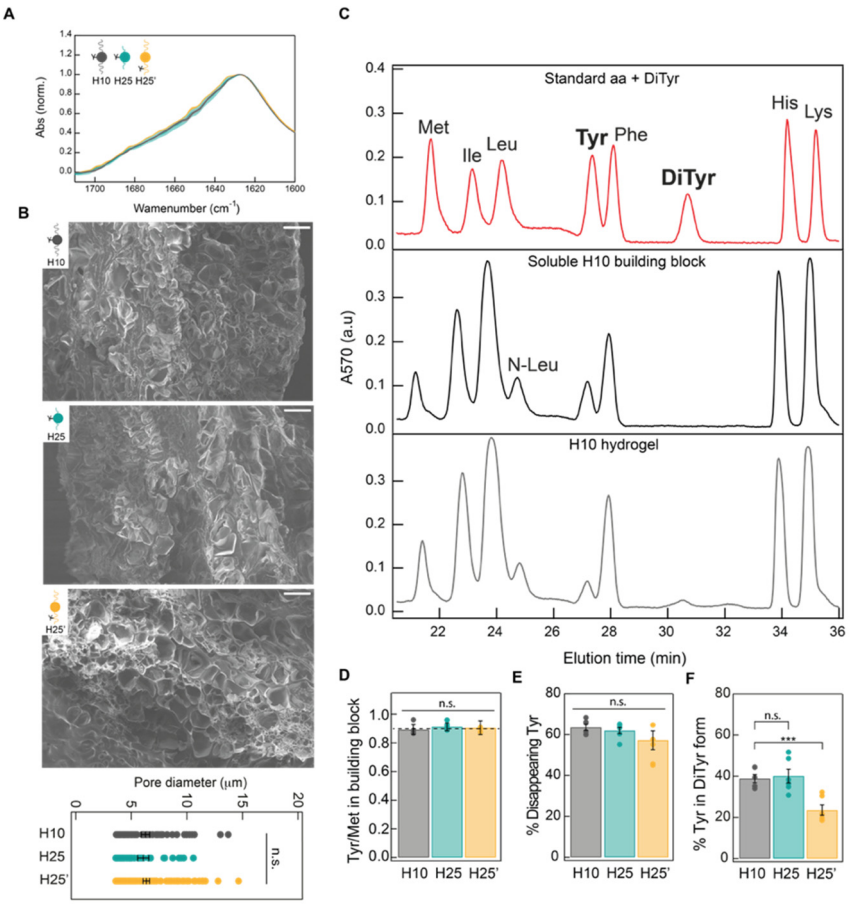

Figure S7: Preservation of non-mechanical properties of H10, H25, and H25' hydrogels. (A) Infrared spectra of H10, H25 and H25' hydrogels. Results represent the average value and SEM of three different determinations. The three hydrogels show overlapping infrared spectra in the amide I region (1700-1600 cm^{-1}), which presents a maximum at 1628 cm^{-1} in agreement with the high β-structure content of the I91 domain [77]. These results indicate similar protein structures in the three hydrogels. Spectra were normalized according to the value at 1628 cm^{-1}. **(B)** Scanning electron microscopy images of H10 (top), H25 (center) and H25' (bottom) hydrogels. Images revealed the formation of a microporous network structure with pore sizes on the scale of a few micrometers, typical of protein hydrogels [79]. Scale bars are 10 µm. Bottom panel shows the quantification of H10, H25, and H25' pore size. Data were obtained from one EM image (45, 73, 103 pores for H10, H25 and H25' hydrogels, respectively, mean ± S.E.M., ordinary one-way analysis of variance (ANOVA), n.s., not significant) **(C)** Amino acids analysis of a mixture of protein amino acids and dityrosine standards (top, red). Amino acid analyses of soluble H10 polyprotein sample (middle, black) and of an H10 hydrogel (bottom, grey). Peaks corresponding to dityrosine are absent in the soluble polyprotein sample while they appear in samples coming from crosslinked hydrogels. **(D)** Experimental tyrosine to methionine ratios are equivalent for the three soluble building blocks and consistent with theoretical values (dotted line). **(E)** Percentage of tyrosines that disappear when soluble polyproteins are crosslinked into hydrogels. **(F)** Proportion of total tyrosines that appear as dityrosine in I91 hydrogels. Data in panels D-F correspond to a n=6 independent hydrogels (Mean ± S.E.M., ANOVA, n.s., not significant, ***$p < 0.0001$).

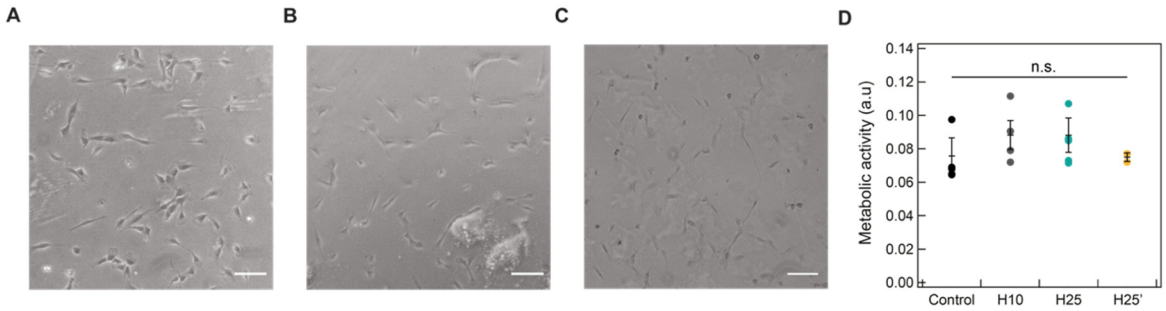

Figure S8: RPE-1 cells are equally metabolically active on H10, H25 and H25' hydrogels. RPE-1 cells grown overnight on **(A)** H10, **(B)** H25 and **(C)** H25' matrices. **(D)** Metabolic activity of RPE-1 cells seeded on the three matrices, as determined by the MTT assay. Cells grown on standard glass coverslips were used as control. Scale bars are 100 µm. n=5 for all conditions except for H25' hydrogels, where n=2. Data are presented as mean ± S.E.M., ordinary one-way analysis of variance (ANOVA), n.s., not significant.

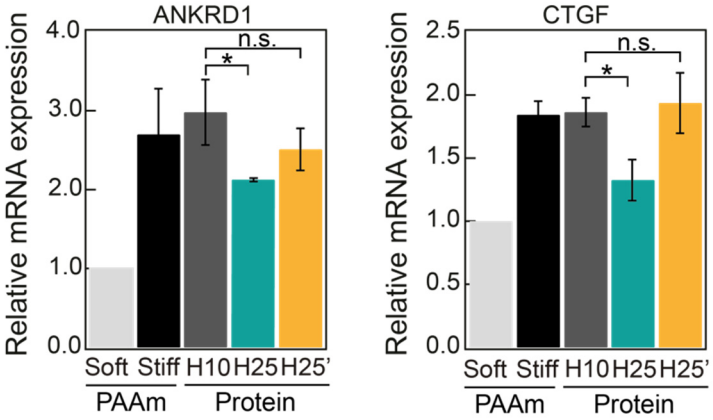

Figure S9: Expression of YAP target genes. mRNA expression levels of YAP target genes ANKRD1 (left) and CTGF (right). n=3 independent experiments except for H25', where n=2. PAAm groups are not considered for statistical analysis. Data are presented as mean ± S.E.M., ordinary one-way analysis of variance (ANOVA), n.s., not significant, *$p<0.05$.

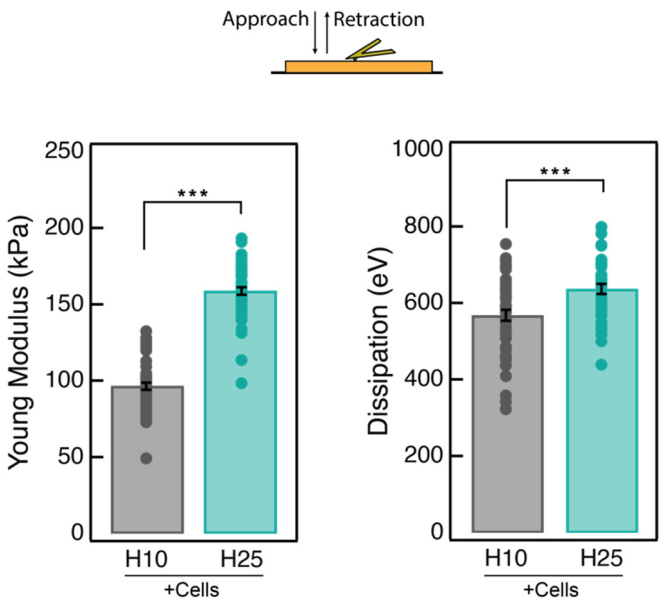

Figure S10: AFM analysis of the nanomechanics of cell-laden I91 hydrogels. Hydrogels were assayed at 10 µm/s after 12 hours of being used as cell substrate at 37 ºC. (N = 10 indentations on 5 positions for one gel, mean ± S.E.M., unpaired two-tailed t-test, ***$p < 0.001$).

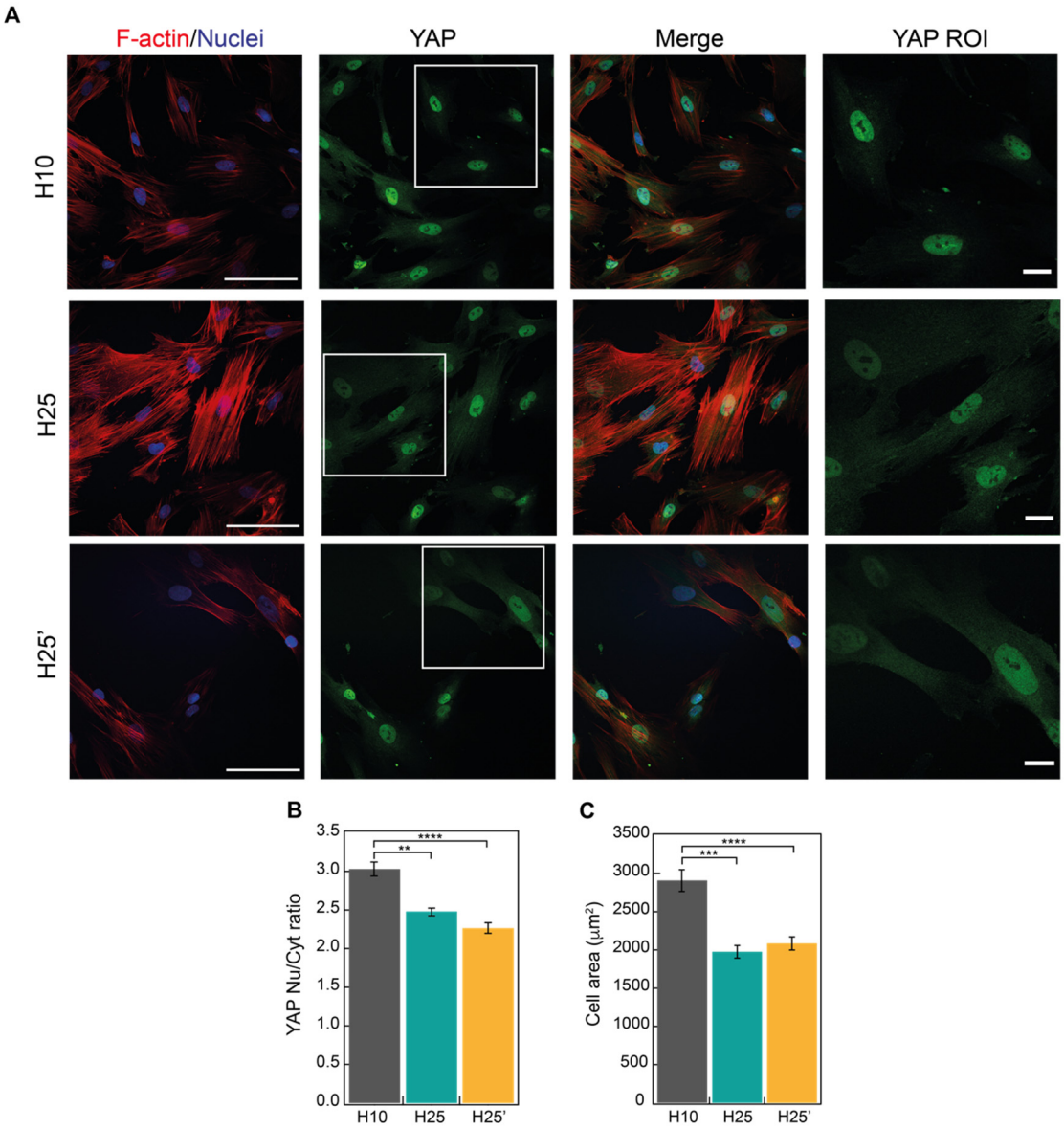

Figure S11: YAP activity in mesenchymal stem cells grown on viscoelastic protein hydrogel matrices. (A) Confocal immunofluorescence images of YAP localization in mesenchymal stem cells grown on different I91 matrices. F-actin was stained with alexa647-conjugated phalloidin (red; left column), and nuclei were stained with DAPI (blue in merged images; first and third column). YAP was labelled with alexa488 conjugated antibody in green (second column). The column on the right shows zoomed views of the YAP ROI (boxed in white in the YAP images). Scale bars are 100 µm (left column) and 20 µm (right column). **(B)** Quantification of YAP distribution. **(C)** Cell spreading quantified as cell area. A minimum of n=30 cells per condition were quantified in a total of 3 independent experiments. Data are presented as mean ± S.E.M., ordinary one-way analysis of variance (ANOVA), ***$p < 0.001$, ****$p < 0.0001$.

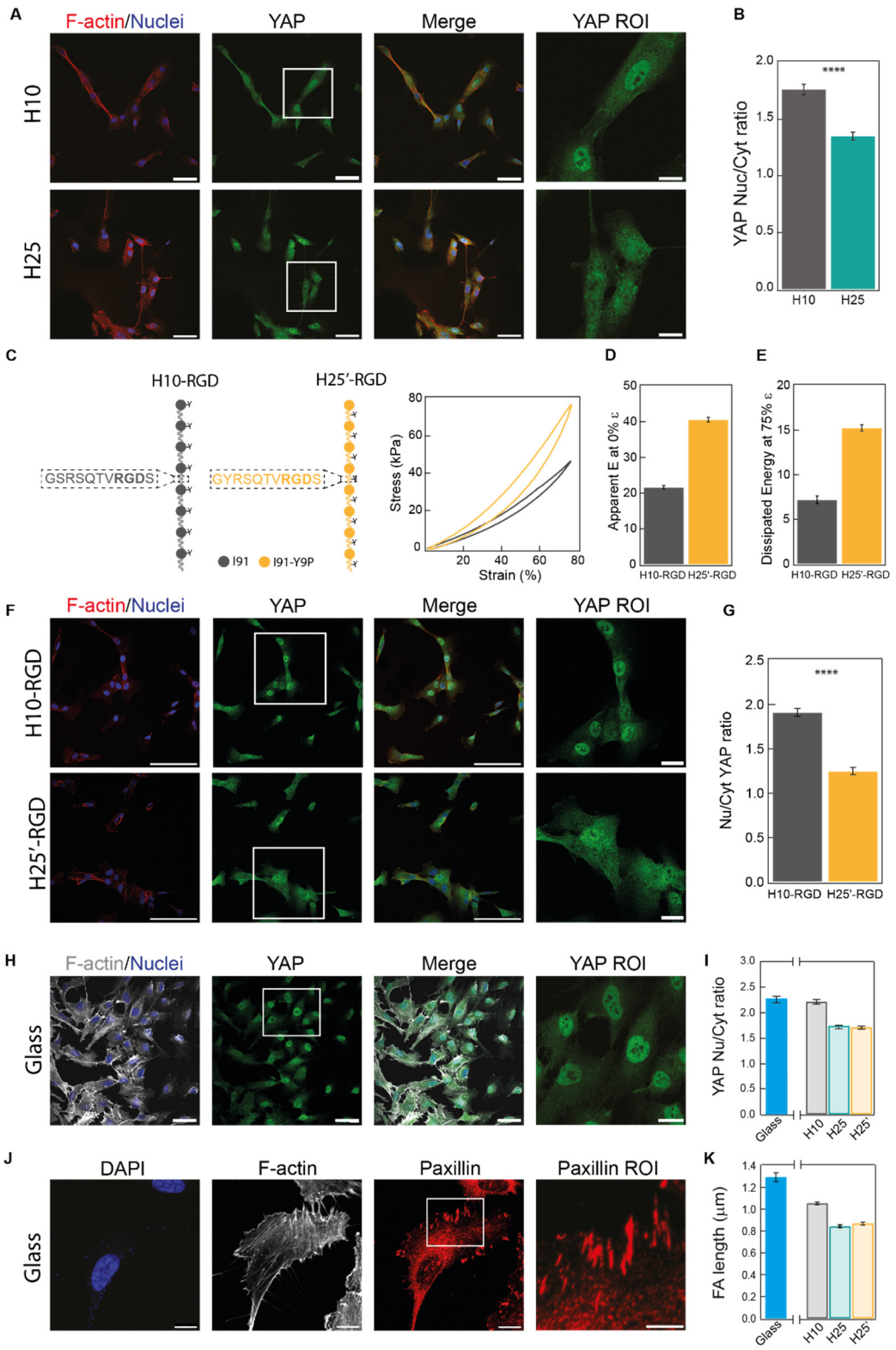

Figure S12. Mechanosensing of cells grown on alternative substrates. (A) Confocal immunofluorescence images of RPE-1 cells grown on H10 and H25 substrates coated with RGD peptide. F-actin was stained with alexa647-phalloidin, and nuclei with DAPI. YAP was labelled with alexa488-conjugated antibody in green. The fourth column shows a ROI of YAP. Scale bars are 100 μm (20 μm ROI). **(B)** Quantification of YAP distribution in RPE-1 grown on substrates coated with RGD peptide. A total of n =162 and n = 140 cells were quantified for H10 and H25 substrates, respectively. (**C**) Schematics of H10-RGD and H25'-

RGD polyproteins with RGD (left) and representative stress-strain curves (right) (**D, E**) Apparent Elastic Moduli at 0% strain (D) and dissipated energy at 75% strain (E) (n=3 from a single protein preparation). (**F**) Confocal images of RPE-1 cells grown on H10-RGD and H25'-RGD substrates (staining as in panel A). (**G**) Quantification of YAP distribution in RPE-1 (n =146 and n = 135 cells for H10-RGD and H25'-RGD , respectively). **(H)** Confocal images of RPE-1 grown on glass (staining as in A). F-actin is shown in grey in first and third column. Scale bars are 100 μm (20 μm ROI). **(I)** Quantification of YAP distribution in cells grown on glass. A total of n=111 cells were quantified. H10, H25 and H25' data are from **Fig. 2C**. **(J)** Confocal images of focal adhesions in RPE-1 grown on glass. Nuclei were stained with DAPI and F-actin was stained with alexa647-phalloidin. Paxillin in focal adhesions was labelled with alexa546-conjugated antibody in red. The fourth column shows a ROI of paxillin. Scale bars are 5 μm. **(K)** Focal adhesion (FA) length quantification. n=10 cells. H10, H25 and H25' data are from **Fig. 2F**. Data are presented as mean ± S.E.M., unpaired two-tailed t-test, ****$p < 0.0001$.

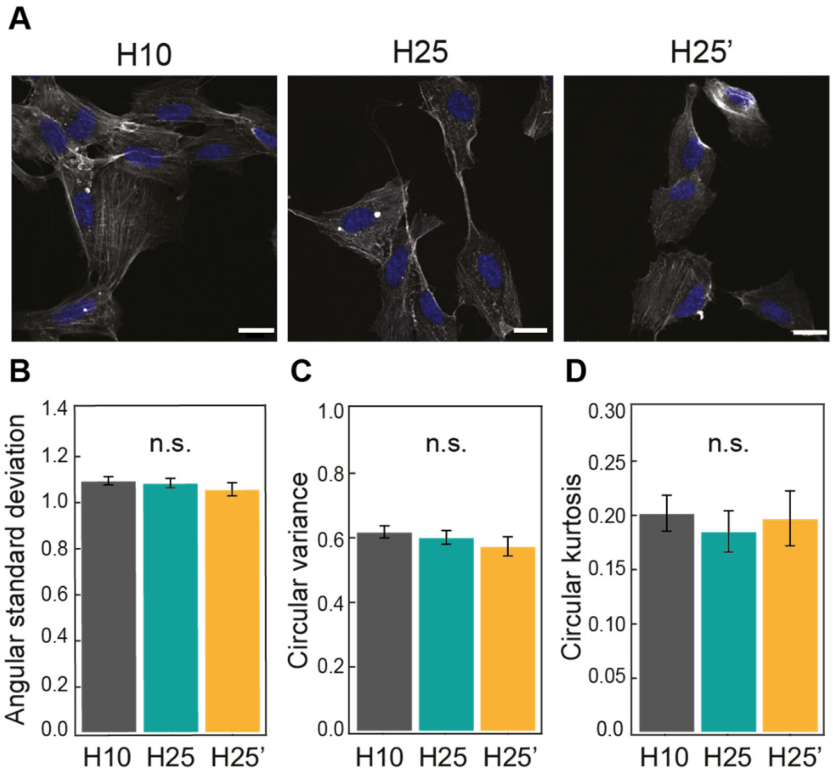

Figure S13. Analysis of actin cytoskeleton organization. (A) Confocal immunofluorescence images of RPE-1 cells grown on I91 hydrogels. Nuclei were stained with DAPI and F-actin was stained with alexa647-conjugated phalloidin. Scale bars are 20 µm. **(B-D)** Analysis of actin cytoskeleton anisotropy by quantification of angular standard deviation (B), circular variance (C) and circular kurtosis (D). Quantification was performed using Cytospectre software. A minimum n = 20 cells per condition were used in the analysis. Data are presented as mean ± S.E.M., ordinary one-way analysis of variance (ANOVA), n.s., not significant.

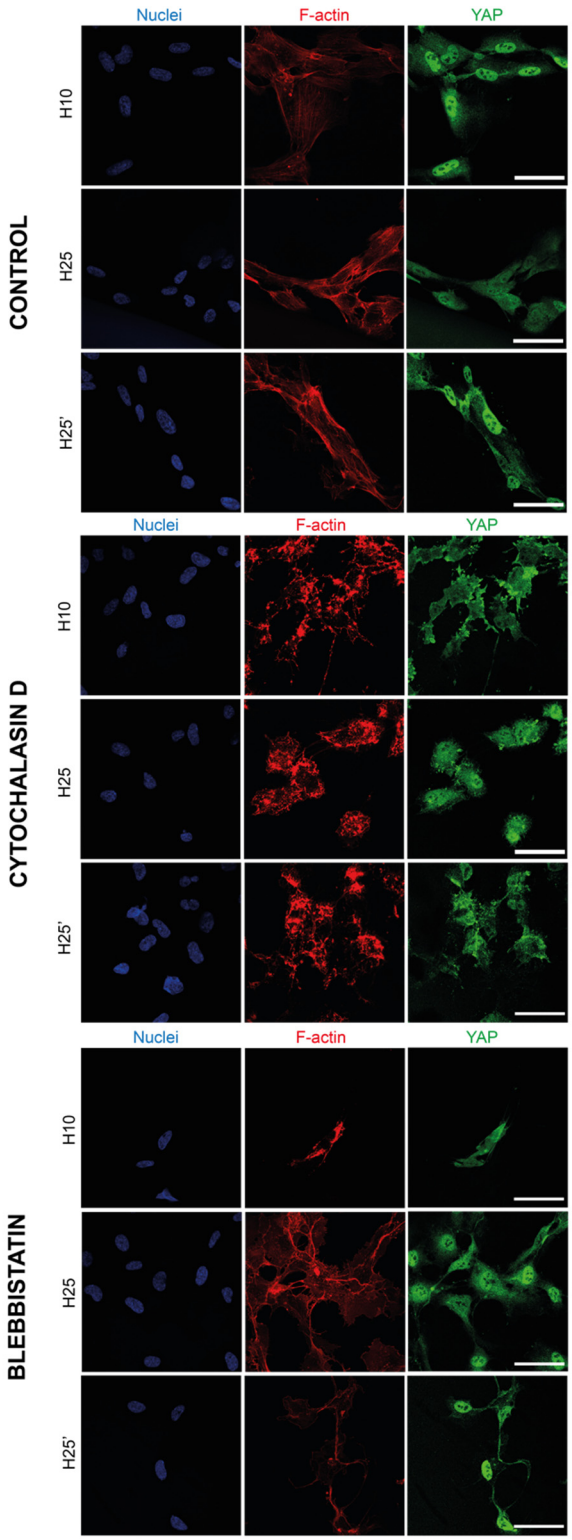

Figure S14: YAP localization in RPE-1 cells grown on viscoelastic protein hydrogel matrices is affected by treatment with actomyosin inhibitors. Confocal immunofluorescence images of YAP localization in RPE-1 cells grown on different I91 matrices and treated with 1 μM cytochalasin D or 10 μM blebbistatin. Nuclei were stained with DAPI (blue; first column). F-actin was stained with alexa647-conjugated phalloidin (red; center column). YAP was labelled with alexa568-conjugated antibody (green; third column). Scale bars are 50 μm.

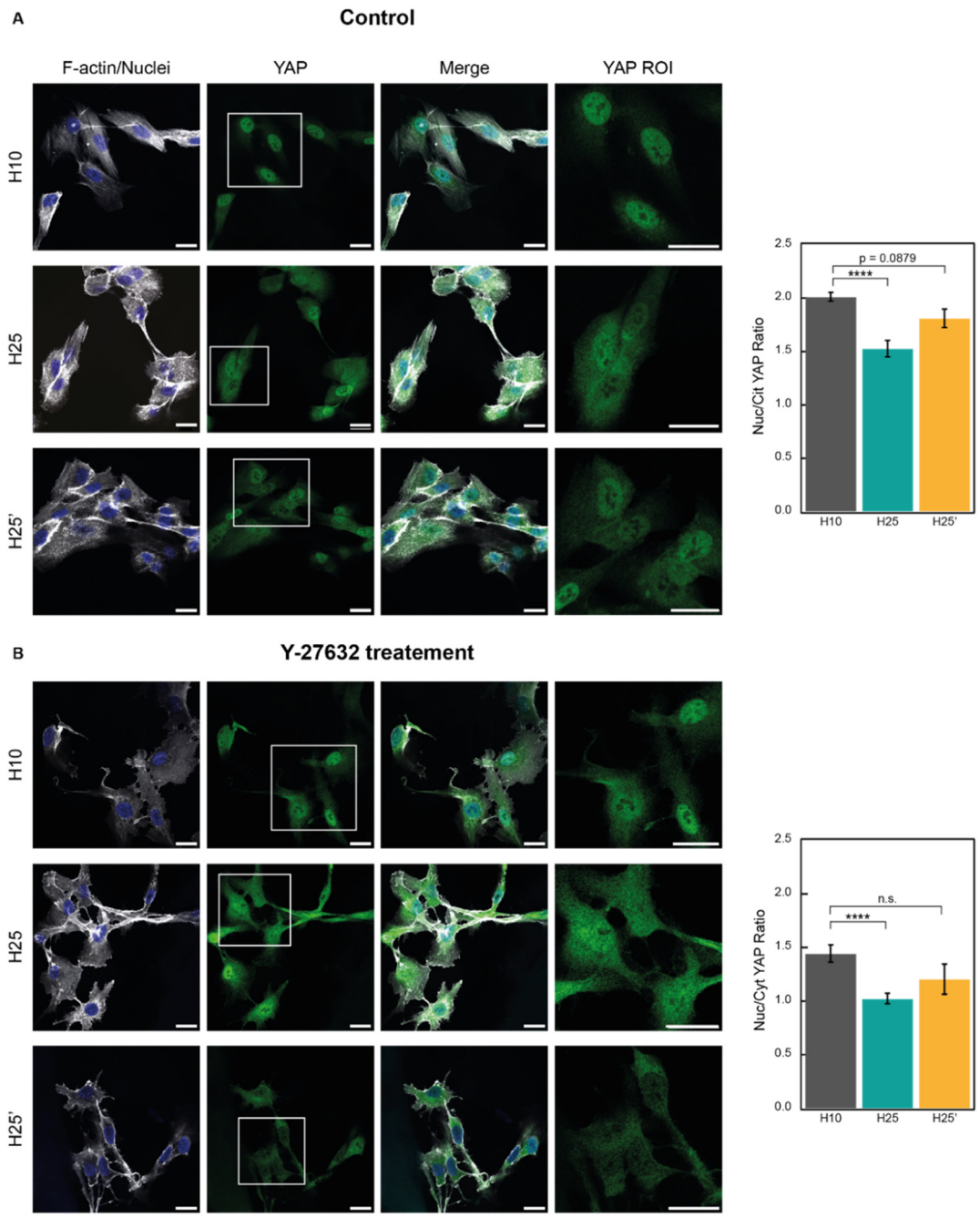

Figure S15. YAP mechanosensing is blunted by Y-27632 treatment. (A) Confocal immunofluorescence images and quantification of YAP localization in RPE-1 cells grown on I91 hydrogels. F-actin was stained with alexa647-conjugated phalloidin (grey in first and third column), and nuclei were stained with DAPI (blue in first and third column). YAP was labelled with alexa488-conjugated antibody in green (second column). The fourth column shows a ROI of the YAP column. Scale bars are 20µm. Data are presented as mean ± S.E.M., ordinary one-way analysis of variance (ANOVA), ****$p < 0.0001$). **(B)** Same as in (A) under 25 µM Y-27632 treatment. Results shown come from a total of 3 independent experiments (at least 42 cells per substrate were analyzed in control conditions and at least 25 cells were analyzed for Y-27632 treatment condition). Data are presented as mean ± S.E.M., ANOVA, n.s., not significant, ****$p < 0.0001$).

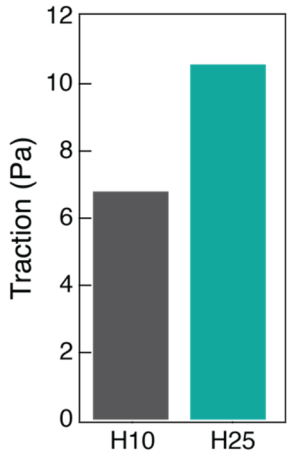

Figure S16. Conventional pull-and-hold molecular clutch model predicts more cell traction on H25-like materials. Maxwell-Wiechert parameters used for the simulations are from **Figure S17**.

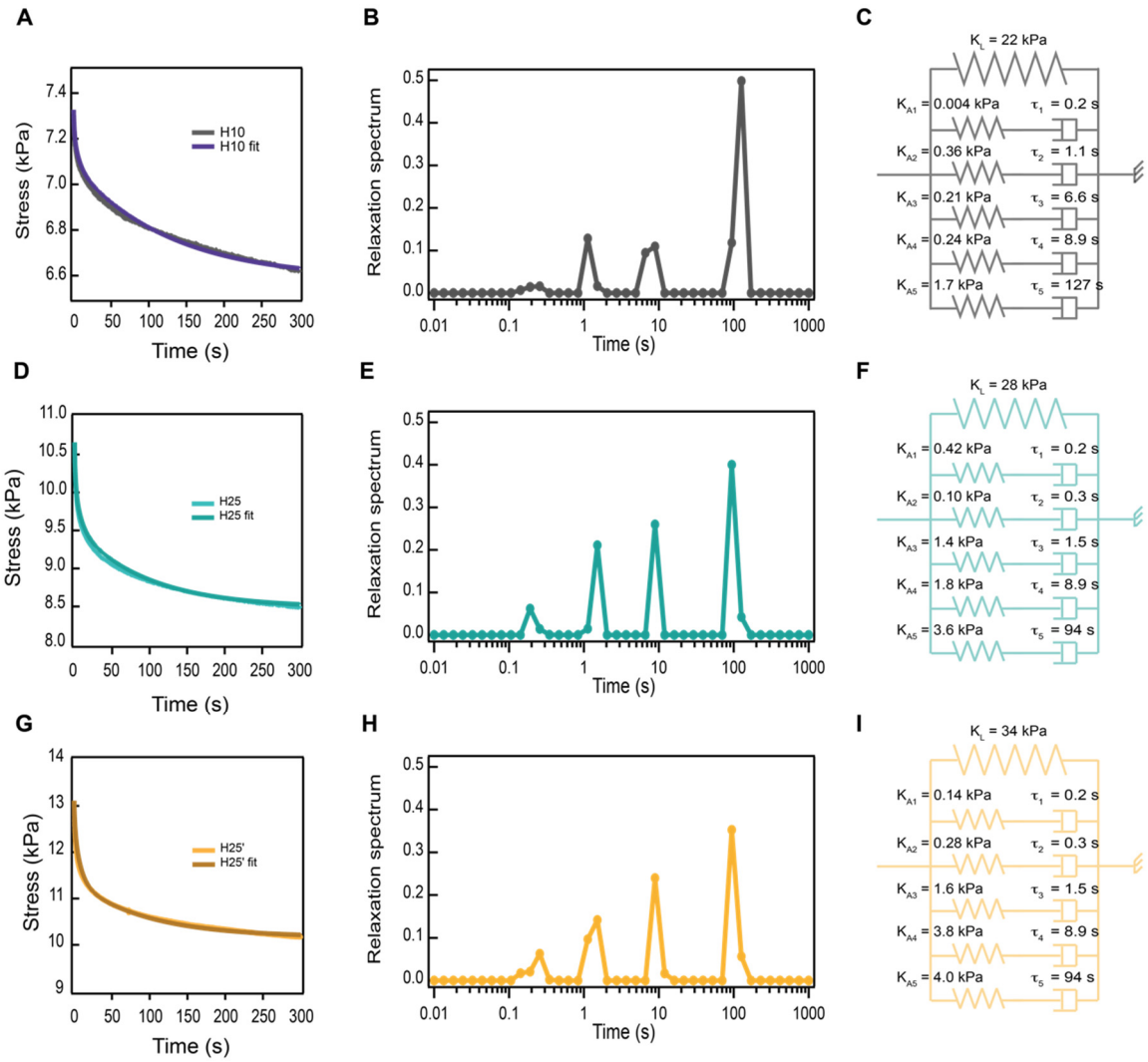

Figure S17. Inverse Laplace transform to extract generalized Maxwell-Wiechert model parameters representing H10, H25 and H25' protein hydrogels (H10-, H25- and H25'-like parameters). (A,B,C) H10 stress-relaxation curve and fit (A) using Laplace transform-based decomposition, and corresponding relaxation spectrum (B) and final fitting parameters (C, total K_A = 2.5 kPa). **(D,E,F)** H25 stress-relaxation curve and fit (D) using Laplace transform-based decomposition, and corresponding relaxation spectrum (E) and final fitting parameters (F, total K_A = 7.3 kPa). **(G,H,I)** H25' stress-relaxation curve and fit (G) using Laplace transform-based decomposition, and corresponding relaxation spectrum (H) and final fitting parameters (I, total K_A = 9.8 kPa). Relaxation curves for H10 and H25 are from Figure 3 (30% strain) cropped at 300 s to allow efficient convergence of the fitting procedure.

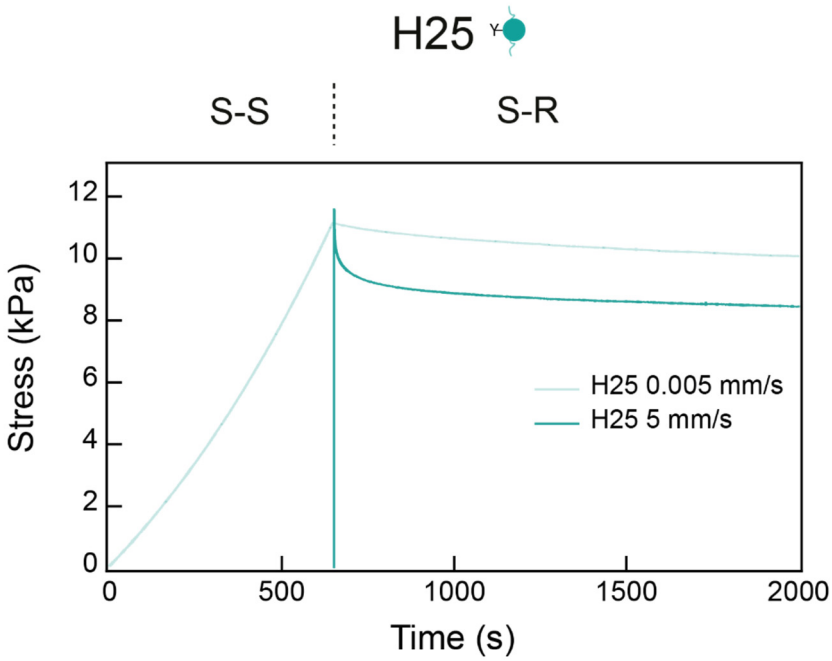

Figure S18. Viscous energy dissipation dependence on pulling speed for H25 hydrogel. (A) Specimens are first stretched in a stress-strain mode (S-S) at a constant pulling speed until a stress value is reached. Afterwards, strain is fixed letting the material relax (stress-relaxation phase, S-R). These tests are performed at 0.005 and 5 mm/s initial pulling speeds.

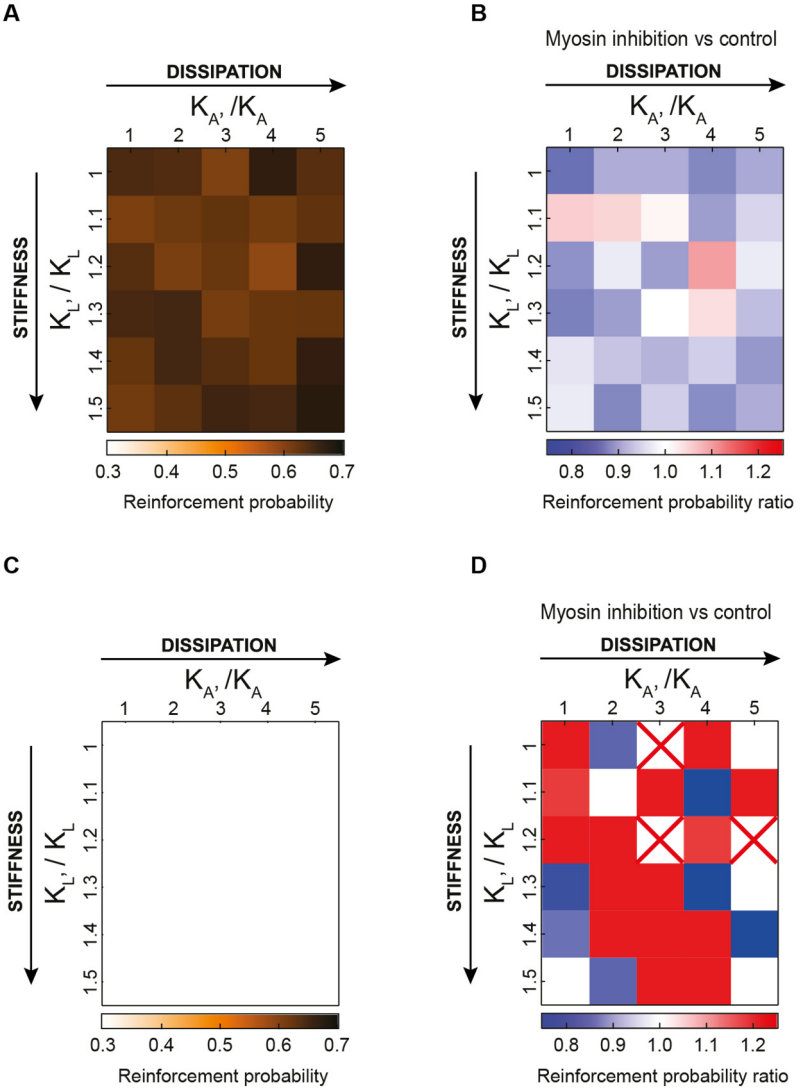

Figure S19. Reinforcement probability from the pull-and-hold model at extreme force thresholds. (A) Reinforcement probability in control conditions using a 15 pN force threshold. **(B)** Reinforcement probability ratio obtained by comparing simulations run at pulling speeds of 0.5 (representing myosin inhibition) and 5 (representing control conditions) % strain per second using a 15 pN force threshold. **(C)** Reinforcement probability in control conditions using a 5 pN force threshold. **(D)** Reinforcement probability ratio obtained by comparing simulations run at pulling speeds of 0.5 (representing myosin inhibition) and 5 (representing control conditions) % strain per second using a 5 pN force threshold. Red crosses represent regions where the ratio could not be calculated due to the very low reinforcement probabilities in these conditions.

Table S1: Sequence of primers used in this study to add adapters to I91-Y9P domain or to follow mRNA expression levels of YAP target genes.

Primer	Sequence
I_27 Y9P Fw	5'-CGCGGATCCGAGACCGTGCGTTTCCAGAGCCTAATAGAAGTGGAAAAGCCTCTGC -3'
I_27 Y9P Rv	5'-ATAGGTACCTTAGCAACAAGATCTATAACCCAATTCTTTCACTTTCAGATTGGCT-3'
CTGF Fw	5'-ACCGACTGGAAGACACGTTTG-3'
CTGF Rv	5'-CCAGGTCAGCTTCGCAAGG-3'
ANKRD 1 Fw	5'-AGTAGAGGAACTGGTCACTGG-3'
ANKRD 1 Rv	5'-TGTTTCTCGCTTTTCCACTGTT-3'
GAPDH Fw	5'-ATCACCATCTTCCAGGAGCG-3'
GAPDH Rv	5'-CCTGCAAATGAGCCCCAG-3'
β-Actin Fw	5'- CACCTTCCAGCAGATGTCGA-3'
β-Actin Rv	5'-AGCATTTGCGGTGGACGATGG-3'

Table S2: Parameters of I91 polyproteins. Parameters were calculated according to ProtParam Tool [80].

Name	Molecular weight (kDa)	Theoretical extinction coefficient ($g \cdot L^{-1} \cdot cm^{-1}$)
H10 (I91 WT)	89.413	0.625
H25 (I91 WT)	81.476	0.686
H25' (I91 Y9P)	89.493	0.625

Table S3: Parameters used in computer simulations.

Parameter	Value	Reference
Integrin's K_{off}	1/150 s^{-1}	(36)
Talin's K_{unfold}	$K_{unfold,\,0} = 2.5 \cdot 10^{-3}\ s^{-1}$, $\Delta x = 6.49$ nm	(35)
Talin's K_{fold}	$K_{fold,\,0} = 1.2 \cdot 10^{-5}\ s^{-1}$, $\Delta x = 4.61$ nm	(35)
[Vinculin]	7.5 nM	(35)
Adhesion's effective area	0.002 μm^2	This manuscript
Montecarlo time interval (Δt)	0.0001 s	

Supplementary Note 1. Sequence of $(I91)_8$ H25 recombinant construct. Sequence including the start codon and a histidine tag used for protein purification is included. BamHI, BglII and BstYI restriction enzymes recognition sequences indicate ligation sites to the expression plasmid and modular assembly between domains, respectively.

BamHI-(I91-BstYI)$_8$-BglII

cDNA:

ATGAGAGGATCGCATCACCATCACCATCACGGATCCCTAATAGAAGTGGAAAAGCCTCTGTACGGAGT
AGAGGTGTTTGTTGGTGAAACAGCCCACTTTGAAATTGAACTTTCTGAACCTGATGTTCACGGCCAGT
GGAAGCTGAAAGGACAGCCTTTGGCAGCTTCCCCTGACTGTGAAATCATTGAGGATGGAAAGAAGCAT
ATTCTGATCCTTCATAACTGTCAGCTGGGTATGACAGGAGAGGTTTCCTTCCAGGCTGCTAATACCAA
ATCTGCAGCCAATCTGAAAGTGAAAGAATTGAGATCCCTAATAGAAGTGGAAAAGCCTCTGTACGGAG
TAGAGGTGTTTGTTGGTGAAACAGCCCACTTTGAAATTGAACTTTCTGAACCTGATGTTCACGGCCAG
TGGAAGCTGAAAGGACAGCCTTTGGCAGCTTCCCCTGACTGTGAAATCATTGAGGATGGAAAGAAGCA
TATTCTGATCCTTCATAACTGTCAGCTGGGTATGACAGGAGAGGTTTCCTTCCAGGCTGCTAATACCA
AATCTGCAGCCAATCTGAAAGTGAAAGAATTGAGATCCCTAATAGAAGTGGAAAAGCCTCTGTACGGA
GTAGAGGTGTTTGTTGGTGAAACAGCCCACTTTGAAATTGAACTTTCTGAACCTGATGTTCACGGCCA
GTGGAAGCTGAAAGGACAGCCTTTGGCAGCTTCCCCTGACTGTGAAATCATTGAGGATGGAAAGAAGC
ATATTCTGATCCTTCATAACTGTCAGCTGGGTATGACAGGAGAGGTTTCCTTCCAGGCTGCTAATACC
AAATCTGCAGCCAATCTGAAAGTGAAAGAATTGAGATCCCTAATAGAAGTGGAAAAGCCTCTGTACGG
AGTAGAGGTGTTTGTTGGTGAAACAGCCCACTTTGAAATTGAACTTTCTGAACCTGATGTTCACGGCC
AGTGGAAGCTGAAAGGACAGCCTTTGGCAGCTTCCCCTGACTGTGAAATCATTGAGGATGGAAAGAAG
CATATTCTGATCCTTCATAACTGTCAGCTGGGTATGACAGGAGAGGTTTCCTTCCAGGCTGCTAATAC
CAAATCTGCAGCCAATCTGAAAGTGAAAGAATTGAGATCCCTAATAGAAGTGGAAAAGCCTCTGTACG
GAGTAGAGGTGTTTGTTGGTGAAACAGCCCACTTTGAAATTGAACTTTCTGAACCTGATGTTCACGGC
CAGTGGAAGCTGAAAGGACAGCCTTTGGCAGCTTCCCCTGACTGTGAAATCATTGAGGATGGAAAGAA
GCATATTCTGATCCTTCATAACTGTCAGCTGGGTATGACAGGAGAGGTTTCCTTCCAGGCTGCTAATA
CCAAATCTGCAGCCAATCTGAAAGTGAAAGAATTGAGATCCCTAATAGAAGTGGAAAAGCCTCTGTAC
GGAGTAGAGGTGTTTGTTGGTGAAACAGCCCACTTTGAAATTGAACTTTCTGAACCTGATGTTCACGG
CCAGTGGAAGCTGAAAGGACAGCCTTTGGCAGCTTCCCCTGACTGTGAAATCATTGAGGATGGAAAGA
AGCATATTCTGATCCTTCATAACTGTCAGCTGGGTATGACAGGAGAGGTTTCCTTCCAGGCTGCTAAT
ACCAAATCTGCAGCCAATCTGAAAGTGAAAGAATTGAGATCCCTAATAGAAGTGGAAAAGCCTCTGTA
CGGAGTAGAGGTGTTTGTTGGTGAAACAGCCCACTTTGAAATTGAACTTTCTGAACCTGATGTTCACG
GCCAGTGGAAGCTGAAAGGACAGCCTTTGGCAGCTTCCCCTGACTGTGAAATCATTGAGGATGGAAAG
AAGCATATTCTGATCCTTCATAACTGTCAGCTGGGTATGACAGGAGAGGTTTCCTTCCAGGCTGCTAA
TACCAAATCTGCAGCCAATCTGAAAGTGAAAGAATTGAGATCCCTAATAGAAGTGGAAAAGCCTCTGT
ACGGAGTAGAGGTGTTTGTTGGTGAAACAGCCCACTTTGAAATTGAACTTTCTGAACCTGATGTTCAC
GGCCAGTGGAAGCTGAAAGGACAGCCTTTGGCAGCTTCCCCTGACTGTGAAATCATTGAGGATGGAAA
GAAGCATATTCTGATCCTTCATAACTGTCAGCTGGGTATGACAGGAGAGGTTTCCTTCCAGGCTGCTA
ATACCAAATCTGCAGCCAATCTGAAAGTGAAAGAATTGAGATCTTAA

Protein:

MRGSHHHHHHGSLIEVEKPLYGVEVFVGETAHFEIELSEPDVHGQWKLKGQPLAASPDCEIIEDGKKH
ILILHNCQLGMTGEVSFQAANTKSAANLKVKELRSLIEVEKPLYGVEVFVGETAHFEIELSEPDVHGQ
WKLKGQPLAASPDCEIIEDGKKHILILHNCQLGMTGEVSFQAANTKSAANLKVKELRSLIEVEKPLYG
VEVFVGETAHFEIELSEPDVHGQWKLKGQPLAASPDCEIIEDGKKHILILHNCQLGMTGEVSFQAANT
KSAANLKVKELRSLIEVEKPLYGVEVFVGETAHFEIELSEPDVHGQWKLKGQPLAASPDCEIIEDGKK
HILILHNCQLGMTGEVSFQAANTKSAANLKVKELRSLIEVEKPLYGVEVFVGETAHFEIELSEPDVHG
QWKLKGQPLAASPDCEIIEDGKKHILILHNCQLGMTGEVSFQAANTKSAANLKVKELRSLIEVEKPLY
GVEVFVGETAHFEIELSEPDVHGQWKLKGQPLAASPDCEIIEDGKKHILILHNCQLGMTGEVSFQAAN
TKSAANLKVKELRSLIEVEKPLYGVEVFVGETAHFEIELSEPDVHGQWKLKGQPLAASPDCEIIEDGK
KHILILHNCQLGMTGEVSFQAANTKSAANLKVKELRSLIEVEKPLYGVEVFVGETAHFEIELSEPDVH
GQWKLKGQPLAASPDCEIIEDGKKHILILHNCQLGMTGEVSFQAANTKSAANLKVKELRS

Supplementary Note 2. Sequence of $(I91)_8$ H10 recombinant construct. Sequence including the start codon providing and a histidine tag used for protein purification is included. BamHI, BglII and BstYI restriction enzymes recognition sequences indicate ligation sites to the expression plasmid and modular assembly between domains, respectively.

BamHI-(linker-I91-GlySer-BstYI)$_8$-BglII

cDNA:

ATGAGAGGATCGCATCACCATCACCATCACGGATCCGAGACCGTGCGTTTCCAGAGCCTAATAGAAGT
GGAAAAGCCTCTGTACGGAGTAGAGGTGTTTGTTGGTGAAACAGCCCACTTTGAAATTGAACTTTCTG
AACCTGATGTTCACGGCCAGTGGAAGCTGAAAGGACAGCCTTTGGCAGCTTCCCCTGACTGTGAAATC
ATTGAGGATGGAAAGAAGCATATTCTGATCCTTCATAACTGTCAGCTGGGTATGACAGGAGAGGTTTC
CTTCCAGGCTGCTAATACCAAATCTGCAGCCAATCTGAAAGTGAAAGAATTGGGTTCTAGATCCGAAA
CCGTTCGCTTTCAGTCACTGATTGAAGTTGAAAAACCGCTGTATGGTGTGGAAGTTTTTGTGGGCGAA
ACCGCACATTTTGAAATCGAGCTGAGCGAACCGGATGTGCATGGTCAATGGAAACTGAAGGGTCAGCC
GCTGGCAGCAAGTCCGGATTGCGAAATTATTGAAGATGGCAAAAAACACATCCTGATTCTGCATAATT
GCCAACTGGGCATGACCGGTGAAGTTAGCTTTCAGGCAGCAAATACAAAAAGCGCTGCAAACCTGAAG
GTTAAAGAACTGGGTAGCCGTAGCGAAACAGTACGTTTTCAGAGTCTGATCGAGGTGGAAAAACCGTT
ATATGGCGTTGAGGTTTTCGTAGGTGAGACTGCCCATTTCGAGATCGAACTGTCAGAGCCAGATGTAC
ATGGACAGTGGAAGTTAAAAGGCCAACCACTGGCAGCATCACCAGATTGTGAGATCATCGAGGACGGT
AAAAAACACATTCTTATCCTGCACAACTGTCAATTAGGTATGACTGGCGAAGTTTCATTTCAAGCAGC
CAATACGAAATCAGCCGCTAACTTAAAAGTAAAAGAGCTGGGTTCACGTTCAGAAACGGTTCGTTTTC
AAAGCCTTATCGAAGTAGAGAAACCACTGTACGGCGTTGAAGTATTCGTTGGAGAAACGGCTCATTTT
GAGATTGAGTTAAGTGAGCCGGACGTTCACGGACAATGGAAATTAAAGGGACAACCGTTAGCCGCTTC
TCCCGATTGTGAAATAATCGAAGATGGGAAGAAACACATTTTGATCTTACACAATTGCCAGTTAGGGA
TGACAGGGGAAGTGAGTTTTCAAGCCGCAAACACCAAAAGTGCAGCGAATTTAAAGGTGAAAGAGTTA
GGTAGCCGCTCAGAAACAGTGAGATTTCAGAGCTTAATTGAGGTTGAGAAACCCCTTTATGGCGTCGA
GGTCTTTGTCGGCGAGACAGCACACTTCGAGATTGAATTATCAGAACCCGACGTGCATGGCCAGTGGA
AACTTAAAGGGCAACCTCTTGCAGCCAGTCCAGACTGCGAGATAATAGAGGACGGCAAGAAGCACATA
TTAATCTTGCATAATTGTCAGCTTGGAATGACTGGTGAAGTGTCGTTCCAGGCAGCGAACACTAAATC
AGCTGCAAATTTGAAAGTCAAAGAACTTGGCAGCCGTTCTGAAACTGTGCGCTTCCAATCTCTTATTG
AGGTAGAAAAGCCGCTTTACGGTGTCGAAGTGTTCGTGGGTGAGACAGCGCATTTTGAAATAGAATTG
TCAGAACCGGATGTACACGGCCAATGGAAGTTAAAGGGTCAGCCGCTTGCCGCATCACCGGACTGTGA
GATTATAGAAGATGGTAAAAAGCATATCTTAATTCTTCACAACTGCCAGCTTGGCATGACTGGCGAGG
TGAGTTTTCAGGCTGCGAATACTAAGAGCGCAGCGAATCTGAAGGTAAAAGAGCTTGGCTCTCGTAGC
GAAACGGTTCGCTTCCAGAGTTTAATTGAAGTCGAGAAGCCGTTATACGGGGTAGAAGTCTTTGTGGG
AGAAACTGCGCACTTTGAGATAGAACTGAGTGAACCAGACGTACACGGTCAGTGGAAGCTTAAGGGGC
AGCCGTTAGCAGCGAGCCCTGATTGCGAGATTATCGAGGATGGGAAAAAGCACATACTGATTTTACAC
AACTGTCAACTGGGAATGACAGGGGAAGTGTCATTTCAAGCGGCAAATACTAAAAGTGCCGCAAATCT
TAAAGTAAAAGAATTAGGTAGTCGCAGCGAAACCGTCAGATTCCAAAGCCTGATAGAGGTCGAGAAGC
CCCTGTATGGGGTTGAAGTGTTCGTAGGCGAAACAGCTCACTTCGAAATCGAGTTATCCGAGCCGGAT
GTCCACGGTCAGTGGAAATTGAAAGGTCAGCCATTAGCAGCGTCACCCGATTGCGAAATCATAGAGGA
TGGGAAAAAACACATCTTAATATTGCATAACTGCCAATTAGGAATGACAGGTGAGGTTAGCTTCCAAG
CGGCAAACACGAAATCCGCTGCCAACTTGAAGGTGAAAGAATTAGGCAGCAGATCTTAA

Protein:

MRGSHHHHHHGSETVRFQSLIEVEKPLYGVEVFVGETAHFEIELSEPDVHGQWKLKGQPLAASPDCEI
IEDGKKHILILHNCQLGMTGEVSFQAANTKSAANLKVKELGSRSETVRFQSLIEVEKPLYGVEVFVGE
TAHFEIELSEPDVHGQWKLKGQPLAASPDCEIIEDGKKHILILHNCQLGMTGEVSFQAANTKSAANLK
VKELGSRSETVRFQSLIEVEKPLYGVEVFVGETAHFEIELSEPDVHGQWKLKGQPLAASPDCEIIEDG
KKHILILHNCQLGMTGEVSFQAANTKSAANLKVKELGSRSETVRFQSLIEVEKPLYGVEVFVGETAHF
EIELSEPDVHGQWKLKGQPLAASPDCEIIEDGKKHILILHNCQLGMTGEVSFQAANTKSAANLKVKEL
GSRSETVRFQSLIEVEKPLYGVEVFVGETAHFEIELSEPDVHGQWKLKGQPLAASPDCEIIEDGKKHI
LILHNCQLGMTGEVSFQAANTKSAANLKVKELGSRSETVRFQSLIEVEKPLYGVEVFVGETAHFEIEL
SEPDVHGQWKLKGQPLAASPDCEIIEDGKKHILILHNCQLGMTGEVSFQAANTKSAANLKVKELGSRS
ETVRFQSLIEVEKPLYGVEVFVGETAHFEIELSEPDVHGQWKLKGQPLAASPDCEIIEDGKKHILILH
NCQLGMTGEVSFQAANTKSAANLKVKELGSRSETVRFQSLIEVEKPLYGVEVFVGETAHFEIELSEPD
VHGQWKLKGQPLAASPDCEIIEDGKKHILILHNCQLGMTGEVSFQAANTKSAANLKVKELGSRS

Supplementary Note 3. Sequence of (I91-Y9P)$_8$ H25' recombinant construct. Sequence including the start codon and a histidine tag used for protein purification is included. BamHI, BglII and BstYI restriction enzymes recognition sequences indicate ligation sites to the expression plasmid and modular assembly between domains, respectively.

BamHI-(linker-I91Y9P-GlyTyr-BstYI)$_8$-BglII

cDNA:

ATGAGAGGATCGCATCACCATCACCATCACGGATCCGAGACCGTGCGTTTCCAGAGCCTAATAGAAGT
GGAAAAGCCTCTGCCGGGAGTAGAGGTGTTTGTTGGTGAAACAGCCCACTTTGAAATTGAACTTTCTG
AACCTGATGTTCACGGCCAGTGGAAGCTGAAAGGACAGCCTTTGGCAGCTTCCCCTGACTGTGAAATC
ATTGAGGATGGAAAGAAGCATATTCTGATCCTTCATAACTGTCAGCTGGGTATGACAGGAGAGGTTTC
CTTCCAGGCTGCTAATACCAAATCTGCAGCCAATCTGAAAGTGAAAGAATTGGGTTATAGATCCGAGA
CCGTGCGTTTCCAGAGCCTAATAGAAGTGGAAAAGCCTCTGCCGGGAGTAGAGGTGTTTGTTGGTGAA
ACAGCCCACTTTGAAATTGAACTTTCTGAACCTGATGTTCACGGCCAGTGGAAGCTGAAAGGACAGCC
TTTGGCAGCTTCCCCTGACTGTGAAATCATTGAGGATGGAAAGAAGCATATTCTGATCCTTCATAACT
GTCAGCTGGGTATGACAGGAGAGGTTTCCTTCCAGGCTGCTAATACCAAATCTGCAGCCAATCTGAAA
GTGAAAGAATTGGGTTATAGATCCGAGACCGTGCGTTTCCAGAGCCTAATAGAAGTGGAAAAGCCTCT
GCCGGGAGTAGAGGTGTTTGTTGGTGAAACAGCCCACTTTGAAATTGAACTTTCTGAACCTGATGTTC
ACGGCCAGTGGAAGCTGAAAGGACAGCCTTTGGCAGCTTCCCCTGACTGTGAAATCATTGAGGATGGA
AAGAAGCATATTCTGATCCTTCATAACTGTCAGCTGGGTATGACAGGAGAGGTTTCCTTCCAGGCTGC
TAATACCAAATCTGCAGCCAATCTGAAAGTGAAAGAATTGGGTTATAGATCCGAGACCGTGCGTTTCC
AGAGCCTAATAGAAGTGGAAAAGCCTCTGCCGGGAGTAGAGGTGTTTGTTGGTGAAACAGCCCACTTT
GAAATTGAACTTTCTGAACCTGATGTTCACGGCCAGTGGAAGCTGAAAGGACAGCCTTTGGCAGCTTC
CCCTGACTGTGAAATCATTGAGGATGGAAAGAAGCATATTCTGATCCTTCATAACTGTCAGCTGGGTA
TGACAGGAGAGGTTTCCTTCCAGGCTGCTAATACCAAATCTGCAGCCAATCTGAAAGTGAAAGAATTG
GGTTATAGATCCGAGACCGTGCGTTTCCAGAGCCTAATAGAAGTGGAAAAGCCTCTGCCGGGAGTAGA
GGTGTTTGTTGGTGAAACAGCCCACTTTGAAATTGAACTTTCTGAACCTGATGTTCACGGCCAGTGGA
AGCTGAAAGGACAGCCTTTGGCAGCTTCCCCTGACTGTGAAATCATTGAGGATGGAAAGAAGCATATT
CTGATCCTTCATAACTGTCAGCTGGGTATGACAGGAGAGGTTTCCTTCCAGGCTGCTAATACCAAATC
TGCAGCCAATCTGAAAGTGAAAGAATTGGGTTATAGATCCGAGACCGTGCGTTTCCAGAGCCTAATAG
AAGTGGAAAAGCCTCTGCCGGGAGTAGAGGTGTTTGTTGGTGAAACAGCCCACTTTGAAATTGAACTT
TCTGAACCTGATGTTCACGGCCAGTGGAAGCTGAAAGGACAGCCTTTGGCAGCTTCCCCTGACTGTGA
AATCATTGAGGATGGAAAGAAGCATATTCTGATCCTTCATAACTGTCAGCTGGGTATGACAGGAGAGG
TTTCCTTCCAGGCTGCTAATACCAAATCTGCAGCCAATCTGAAAGTGAAAGAATTGGGTTATAGATCC
GAGACCGTGCGTTTCCAGAGCCTAATAGAAGTGGAAAAGCCTCTGCCGGGAGTAGAGGTGTTTGTTGG
TGAAACAGCCCACTTTGAAATTGAACTTTCTGAACCTGATGTTCACGGCCAGTGGAAGCTGAAAGGAC
AGCCTTTGGCAGCTTCCCCTGACTGTGAAATCATTGAGGATGGAAAGAAGCATATTCTGATCCTTCAT
AACTGTCAGCTGGGTATGACAGGAGAGGTTTCCTTCCAGGCTGCTAATACCAAATCTGCAGCCAATCT
GAAAGTGAAAGAATTGGGTTATAGATCCGAGACCGTGCGTTTCCAGAGCCTAATAGAAGTGGAAAAGC
CTCTGCCGGGAGTAGAGGTGTTTGTTGGTGAAACAGCCCACTTTGAAATTGAACTTTCTGAACCTGAT
GTTCACGGCCAGTGGAAGCTGAAAGGACAGCCTTTGGCAGCTTCCCCTGACTGTGAAATCATTGAGGA
TGGAAAGAAGCATATTCTGATCCTTCATAACTGTCAGCTGGGTATGACAGGAGAGGTTTCCTTCCAGG
CTGCTAATACCAAATCTGCAGCCAATCTGAAAGTGAAAGAATTGGGTTATAGATCTTAA

Protein:

MRGSHHHHHHGSETVRFQSLIEVEKPLPGVEVFVGETAHFEIELSEPDVHGQWKLKGQPLAASPDCEI
IEDGKKHILILHNCQLGMTGEVSFQAANTKSAANLKVKELGYRSETVRFQSLIEVEKPLPGVEVFVGE
TAHFEIELSEPDVHGQWKLKGQPLAASPDCEIIEDGKKHILILHNCQLGMTGEVSFQAANTKSAANLK
VKELGYRSETVRFQSLIEVEKPLPGVEVFVGETAHFEIELSEPDVHGQWKLKGQPLAASPDCEIIEDG
KKHILILHNCQLGMTGEVSFQAANTKSAANLKVKELGYRSETVRFQSLIEVEKPLPGVEVFVGETAHF
EIELSEPDVHGQWKLKGQPLAASPDCEIIEDGKKHILILHNCQLGMTGEVSFQAANTKSAANLKVKEL
GYRSETVRFQSLIEVEKPLPGVEVFVGETAHFEIELSEPDVHGQWKLKGQPLAASPDCEIIEDGKKHI
LILHNCQLGMTGEVSFQAANTKSAANLKVKELGYRSETVRFQSLIEVEKPLPGVEVFVGETAHFEIEL
SEPDVHGQWKLKGQPLAASPDCEIIEDGKKHILILHNCQLGMTGEVSFQAANTKSAANLKVKELGYRS
ETVRFQSLIEVEKPLPGVEVFVGETAHFEIELSEPDVHGQWKLKGQPLAASPDCEIIEDGKKHILILH
NCQLGMTGEVSFQAANTKSAANLKVKELGYRSETVRFQSLIEVEKPLPGVEVFVGETAHFEIELSEPD
VHGQWKLKGQPLAASPDCEIIEDGKKHILILHNCQLGMTGEVSFQAANTKSAANLKVKELGYRS

Supplementary Note 4. Sequence of (I91)$_8$ H10-RGD recombinant construct. Sequence including the start codon providing and a histidine tag used for protein purification is included. BamHI, BglII and BstYI restriction enzymes recognition sequences indicate ligation sites to the expression plasmid and modular assembly between domains, respectively. Residues modified to include the RGD motif are highlighted in yellow. Please note that the total charge of the construct is preserved by mutating the glutamic acid residue in the targeted linker to glutamine.

BamHI-(linker-I91-GlySer-BstYI)$_8$-BglII

cDNA:

ATGAGAGGATCGCATCACCATCACCATCACGGATCCGAGACCGTGCGTTTCCAGAGCCTAATAGAAGT
GGAAAAGCCTCTGTACGGAGTAGAGGTGTTTGTTGGTGAAACAGCCCACTTTGAAATTGAACTTTCTG
AACCTGATGTTCACGGCCAGTGGAAGCTGAAAGGACAGCCTTTGGCAGCTTCCCCTGACTGTGAAATC
ATTGAGGATGGAAAGAAGCATATTCTGATCCTTCATAACTGTCAGCTGGGTATGACAGGAGAGGTTTC
CTTCCAGGCTGCTAATACCAAATCTGCAGCCAATCTGAAAGTGAAAGAATTGGGTTCTAGATCCGAAA
CCGTTCGCTTTCAGTCACTGATTGAAGTTGAAAAACCGCTGTATGGTGTGGAAGTTTTTGTGGGCGAA
ACCGCACATTTTGAAATCGAGCTGAGCGAACCGGATGTGCATGGTCAATGGAAACTGAAGGGTCAGCC
GCTGGCAGCAAGTCCGGATTGCGAAATTATTGAAGATGGCAAAAAACACATCCTGATTCTGCATAATT
GCCAACTGGGCATGACCGGTGAAGTTAGCTTTCAGGCAGCAAATACAAAAAGCGCTGCAAACCTGAAG
GTTAAAGAACTGGGTAGCCGTAGCGAAACAGTACGTTTTCAGAGTCTGATCGAGGTGGAAAAACCGTT
ATATGGCGTTGAGGTTTTCGTAGGTGAGACTGCCCATTTCGAGATCGAACTGTCAGAGCCAGATGTAC
ATGGACAGTGGAAGTTAAAAGGCCAACCACTGGCAGCATCACCAGATTGTGAGATCATCGAGGACGGT
AAAAAACACATTCTTATCCTGCACAACTGTCAATTAGGTATGACTGGCGAAGTTTCATTTCAAGCAGC
CAATACGAAATCAGCCGCTAACTTAAAAGTAAAAGAGCTGGGTTCACGTTCAGAAACGGTTCGTTTTC
AAAGCCTTATCGAAGTAGAGAAACCACTGTACGGCGTTGAAGTATTCGTTGGAGAAACGGCTCATTTT
GAGATTGAGTTAAGTGAGCCGGACGTTCACGGACAATGGAAATTAAAGGGACAACCGTTAGCCGCTTC
TCCCGATTGTGAAATAATCGAAGATGGGAAGAAACACATTTTGATCTTACACAATTGCCAGTTAGGGA
TGACAGGGGAAGTGAGTTTTCAAGCCGCAAACACCAAAAGTGCAGCGAATTTAAAGGTGAAAGAGTTA
GGTAGCCGCTCACAAACAGTGAGAGGTGACAGCTTAATTGAGGTTGAGAAACCCCTTTATGGCGTCGA
GGTCTTTGTCGGCGAGACAGCACACTTCGAGATTGAATTATCAGAACCCGACGTGCATGGCCAGTGGA
AACTTAAAGGGCAACCTCTTGCAGCCAGTCCAGACTGCGAGATAATAGAGGACGGCAAGAAGCACATA
TTAATCTTGCATAATTGTCAGCTTGGAATGACTGGTGAAGTGTCGTTCCAGGCAGCGAACACTAAATC
AGCTGCAAATTTGAAAGTCAAAGAACTTGGCAGCCGTTCTGAAACTGTGCGCTTCCAATCTCTTATTG
AGGTAGAAAAGCCGCTTTACGGTGTCGAAGTGTTCGTGGGTGAGACAGCGCATTTTGAAATAGAATTG
TCAGAACCGGATGTACACGGCCAATGGAAGTTAAAGGGTCAGCCGCTTGCCGCATCACCGGACTGTGA
GATTATAGAAGATGGTAAAAAGCATATCTTAATTCTTCACAACTGCCAGCTTGGCATGACTGGCGAGG
TGAGTTTTCAGGCTGCGAATACTAAGAGCGCAGCGAATCTGAAGGTAAAAGAGCTTGGCTCTCGTAGC
GAAACGGTTCGCTTCCAGAGTTTAATTGAAGTCGAGAAGCCGTTATACGGGGTAGAAGTCTTTGTGGG
AGAAACTGCGCACTTTGAGATAGAACTGAGTGAACCAGACGTACACGGTCAGTGGAAGCTTAAGGGGC
AGCCGTTAGCAGCGAGCCCTGATTGCGAGATTATCGAGGATGGGAAAAAGCACATACTGATTTTACAC
AACTGTCAACTGGGAATGACAGGGGAAGTGTCATTTCAAGCGGCAAATACTAAAAGTGCCGCAAATCT
TAAAGTAAAAGAATTAGGTAGTCGCAGCGAAACCGTCAGATTCCAAAGCCTGATAGAGGTCGAGAAGC
CCCTGTATGGGGTTGAAGTGTTCGTAGGCGAAACAGCTCACTTCGAAATCGAGTTATCCGAGCCGGAT
GTCCACGGTCAGTGGAAATTGAAAGGTCAGCCATTAGCAGCGTCACCCGATTGCGAAATCATAGAGGA
TGGGAAAAAACACATCTTAATATTGCATAACTGCCAATTAGGAATGACAGGTGAGGTTAGCTTCCAAG
CGGCAAACACGAAATCCGCTGCCAACTTGAAGGTGAAAGAATTAGGCAGCAGATCTTAA

Protein:

MRGSHHHHHHGSETVRFQSLIEVEKPLYGVEVFVGETAHFEIELSEPDVHGQWKLKGQPLAASPDCEI
IEDGKKHILILHNCQLGMTGEVSFQAANTKSAANLKVKELGSRSETVRFQSLIEVEKPLYGVEVFVGE
TAHFEIELSEPDVHGQWKLKGQPLAASPDCEIIEDGKKHILILHNCQLGMTGEVSFQAANTKSAANLK
VKELGSRSETVRFQSLIEVEKPLYGVEVFVGETAHFEIELSEPDVHGQWKLKGQPLAASPDCEIIEDG
KKHILILHNCQLGMTGEVSFQAANTKSAANLKVKELGSRSETVRFQSLIEVEKPLYGVEVFVGETAHF
EIELSEPDVHGQWKLKGQPLAASPDCEIIEDGKKHILILHNCQLGMTGEVSFQAANTKSAANLKVKEL
GSRSQTVRGDSLIEVEKPLYGVEVFVGETAHFEIELSEPDVHGQWKLKGQPLAASPDCEIIEDGKKHI
LILHNCQLGMTGEVSFQAANTKSAANLKVKELGSRSETVRFQSLIEVEKPLYGVEVFVGETAHFEIEL
SEPDVHGQWKLKGQPLAASPDCEIIEDGKKHILILHNCQLGMTGEVSFQAANTKSAANLKVKELGSRS
ETVRFQSLIEVEKPLYGVEVFVGETAHFEIELSEPDVHGQWKLKGQPLAASPDCEIIEDGKKHILILH
NCQLGMTGEVSFQAANTKSAANLKVKELGSRSETVRFQSLIEVEKPLYGVEVFVGETAHFEIELSEPD
VHGQWKLKGQPLAASPDCEIIEDGKKHILILHNCQLGMTGEVSFQAANTKSAANLKVKELGSRS

Supplementary Note 5. Sequence of (I91-Y9P)$_8$ H25'-RGD recombinant construct. Sequence including the start codon and a histidine tag used for protein purification is included. BamHI, BglII and BstYI restriction enzymes recognition sequences indicate ligation sites to the expression plasmid and modular assembly between domains, respectively. Residues modified to include the RGD motif are highlighted in yellow. Please note that the total charge of the construct is preserved by mutating the glutamic acid residue in the targeted linker to glutamine.

BamHI-(linker-I91Y9P-GlyTyr-BstYI)$_8$-BglII

cDNA:

ATGAGAGGATCGCATCACCATCACCATCACGGATCCGAGACCGTGCGTTTCCAGAGCCTAATAGAAGT
GGAAAAGCCTCTGCCGGGAGTAGAGGTGTTTGTTGGTGAAACAGCCCACTTTGAAATTGAACTTTCTG
AACCTGATGTTCACGGCCAGTGGAAGCTGAAAGGACAGCCTTTGGCAGCTTCCCCTGACTGTGAAATC
ATTGAGGATGGAAAGAAGCATATTCTGATCCTTCATAACTGTCAGCTGGGTATGACAGGAGAGGTTTC
CTTCCAGGCTGCTAATACCAAATCTGCAGCCAATCTGAAAGTGAAAGAATTGGGTTATAGATCCGAGA
CCGTGCGTTTCCAGAGCCTAATAGAAGTGGAAAAGCCTCTGCCGGGAGTAGAGGTGTTTGTTGGTGAA
ACAGCCCACTTTGAAATTGAACTTTCTGAACCTGATGTTCACGGCCAGTGGAAGCTGAAAGGACAGCC
TTTGGCAGCTTCCCCTGACTGTGAAATCATTGAGGATGGAAAGAAGCATATTCTGATCCTTCATAACT
GTCAGCTGGGTATGACAGGAGAGGTTTCCTTCCAGGCTGCTAATACCAAATCTGCAGCCAATCTGAAA
GTGAAAGAATTGGGTTATAGATCCGAGACCGTGCGTTTCCAGAGCCTAATAGAAGTGGAAAAGCCTCT
GCCGGGAGTAGAGGTGTTTGTTGGTGAAACAGCCCACTTTGAAATTGAACTTTCTGAACCTGATGTTC
ACGGCCAGTGGAAGCTGAAAGGACAGCCTTTGGCAGCTTCCCCTGACTGTGAAATCATTGAGGATGGA
AAGAAGCATATTCTGATCCTTCATAACTGTCAGCTGGGTATGACAGGAGAGGTTTCCTTCCAGGCTGC
TAATACCAAATCTGCAGCCAATCTGAAAGTGAAAGAATTGGGTTATAGATCCGAGACCGTGCGTTTCC
AGAGCCTAATAGAAGTGGAAAAGCCTCTGCCGGGAGTAGAGGTGTTTGTTGGTGAAACAGCCCACTTT
GAAATTGAACTTTCTGAACCTGATGTTCACGGCCAGTGGAAGCTGAAAGGACAGCCTTTGGCAGCTTC
CCCTGACTGTGAAATCATTGAGGATGGAAAGAAGCATATTCTGATCCTTCATAACTGTCAGCTGGGTA
TGACAGGAGAGGTTTCCTTCCAGGCTGCTAATACCAAATCTGCAGCCAATCTGAAAGTGAAAGAATTG
GGTTATAGATCCCAGACCGTGCGTGGCGACAGCCTAATAGAAGTGGAAAAGCCTCTGCCGGGAGTAGA
GGTGTTTGTTGGTGAAACAGCCCACTTTGAAATTGAACTTTCTGAACCTGATGTTCACGGCCAGTGGA
AGCTGAAAGGACAGCCTTTGGCAGCTTCCCCTGACTGTGAAATCATTGAGGATGGAAAGAAGCATATT
CTGATCCTTCATAACTGTCAGCTGGGTATGACAGGAGAGGTTTCCTTCCAGGCTGCTAATACCAAATC
TGCAGCCAATCTGAAAGTGAAAGAATTGGGTTATAGATCCGAGACCGTGCGTTTCCAGAGCCTAATAG
AAGTGGAAAAGCCTCTGCCGGGAGTAGAGGTGTTTGTTGGTGAAACAGCCCACTTTGAAATTGAACTT
TCTGAACCTGATGTTCACGGCCAGTGGAAGCTGAAAGGACAGCCTTTGGCAGCTTCCCCTGACTGTGA
AATCATTGAGGATGGAAAGAAGCATATTCTGATCCTTCATAACTGTCAGCTGGGTATGACAGGAGAGG
TTTCCTTCCAGGCTGCTAATACCAAATCTGCAGCCAATCTGAAAGTGAAAGAATTGGGTTATAGATCC
GAGACCGTGCGTTTCCAGAGCCTAATAGAAGTGGAAAAGCCTCTGCCGGGAGTAGAGGTGTTTGTTGG
TGAAACAGCCCACTTTGAAATTGAACTTTCTGAACCTGATGTTCACGGCCAGTGGAAGCTGAAAGGAC
AGCCTTTGGCAGCTTCCCCTGACTGTGAAATCATTGAGGATGGAAAGAAGCATATTCTGATCCTTCAT
AACTGTCAGCTGGGTATGACAGGAGAGGTTTCCTTCCAGGCTGCTAATACCAAATCTGCAGCCAATCT
GAAAGTGAAAGAATTGGGTTATAGATCCGAGACCGTGCGTTTCCAGAGCCTAATAGAAGTGGAAAAGC
CTCTGCCGGGAGTAGAGGTGTTTGTTGGTGAAACAGCCCACTTTGAAATTGAACTTTCTGAACCTGAT
GTTCACGGCCAGTGGAAGCTGAAAGGACAGCCTTTGGCAGCTTCCCCTGACTGTGAAATCATTGAGGA
TGGAAAGAAGCATATTCTGATCCTTCATAACTGTCAGCTGGGTATGACAGGAGAGGTTTCCTTCCAGG
CTGCTAATACCAAATCTGCAGCCAATCTGAAAGTGAAAGAATTGGGTTATAGATCTTAA

Protein:

MRGSHHHHHHGSETVRFQSLIEVEKPLPGVEVFVGETAHFEIELSEPDVHGQWKLKGQPLAASPDCEI
IEDGKKHILILHNCQLGMTGEVSFQAANTKSAANLKVKELGYRSETVRFQSLIEVEKPLPGVEVFVGE
TAHFEIELSEPDVHGQWKLKGQPLAASPDCEIIEDGKKHILILHNCQLGMTGEVSFQAANTKSAANLK
VKELGYRSETVRFQSLIEVEKPLPGVEVFVGETAHFEIELSEPDVHGQWKLKGQPLAASPDCEIIEDG
KKHILILHNCQLGMTGEVSFQAANTKSAANLKVKELGYRSETVRFQSLIEVEKPLPGVEVFVGETAHF
EIELSEPDVHGQWKLKGQPLAASPDCEIIEDGKKHILILHNCQLGMTGEVSFQAANTKSAANLKVKEL
GYRSQTVRGDSLIEVEKPLPGVEVFVGETAHFEIELSEPDVHGQWKLKGQPLAASPDCEIIEDGKKHI
LILHNCQLGMTGEVSFQAANTKSAANLKVKELGYRSETVRFQSLIEVEKPLPGVEVFVGETAHFEIEL
SEPDVHGQWKLKGQPLAASPDCEIIEDGKKHILILHNCQLGMTGEVSFQAANTKSAANLKVKELGYRS
ETVRFQSLIEVEKPLPGVEVFVGETAHFEIELSEPDVHGQWKLKGQPLAASPDCEIIEDGKKHILILH
NCQLGMTGEVSFQAANTKSAANLKVKELGYRSETVRFQSLIEVEKPLPGVEVFVGETAHFEIELSEPD
VHGQWKLKGQPLAASPDCEIIEDGKKHILILHNCQLGMTGEVSFQAANTKSAANLKVKELGYRS

Supplementary File 1 (available online). Simulation code. Simulation code for the single-chain, pull-and-hold model of cell mechanosensing.

REFERENCES AND NOTES

1. C. Bonnans, J. Chou, Z. Werb, Remodelling the extracellular matrix in development and disease. *Nat. Rev. Mol. Cell. Biol.* **15**, 786–801 (2014).

2. J. D. Humphrey, E. R. Dufresne, M. A. Schwartz, Mechanotransduction and extracellular matrix homeostasis. *Nat. Rev. Mol. Cell. Biol.* **15**, 802–812 (2014).

3. A. J. Engler, S. Sen, H. L. Sweeney, D. E. Discher, Matrix elasticity directs stem cell lineage specification. *Cell* **126**, 677–689 (2006).

4. A. Elosegui-Artola, X. Trepat, P. Roca-Cusachs, Control of mechanotransduction by molecular clutch dynamics. *Trends Cell Biol.* **28**, 356–367 (2018).

5. M. Segel, B. Neumann, M. F. E. Hill, I. P. Weber, C. Viscomi, C. Zhao, A. Young, C. C. Agley, A. J. Thompson, G. A. Gonzalez, A. Sharma, S. Holmqvist, D. H. Rowitch, K. Franze, R. J. M. Franklin, K. J. Chalut, Niche stiffness underlies the ageing of central nervous system progenitor cells. *Nature* **573**, 130–134 (2019).

6. M. J. Paszek, N. Zahir, K. R. Johnson, J. N. Lakins, G. I. Rozenberg, A. Gefen, C. A. Reinhart-King, S. S. Margulies, M. Dembo, D. Boettiger, D. A. Hammer, V. M. Weaver, Tensional homeostasis and the malignant phenotype. *Cancer Cell* **8**, 241–254 (2005).

7. H. Chen, J. Qu, X. Huang, A. Kurundkar, L. Zhu, N. Yang, A. Venado, Q. Ding, G. Liu, V. B. Antony, V. J. Thannickal, Y. Zhou, Mechanosensing by the α6-integrin confers an invasive fibroblast phenotype and mediates lung fibrosis. *Nat. Commun.* **7**, 12564 (2016).

8. S. Dupont, L. Morsut, M. Aragona, E. Enzo, S. Giulitti, M. Cordenonsi, F. Zanconato, J. Le Digabel, M. Forcato, S. Bicciato, N. Elvassore, S. Piccolo, Role of YAP/TAZ in mechanotransduction. *Nature* **474**, 179–183 (2011).

9. G. Brusatin, T. Panciera, A. Gandin, A. Citron, S. Piccolo, Biomaterials and engineered microenvironments to control YAP/TAZ-dependent cell behaviour. *Nat. Mater.* **17**, 1063–1075 (2018).

10. A. Elosegui-Artola, R. Oria, Y. Chen, A. Kosmalska, C. Perez-Gonzalez, N. Castro, C. Zhu, X. Trepat, P. Roca-Cusachs, Mechanical regulation of a molecular clutch defines force transmission and transduction in response to matrix rigidity. *Nat. Cell Biol.* **18**, 540–548 (2016).

11. A. R. Cameron, J. E. Frith, J. J. Cooper-White, The influence of substrate creep on mesenchymal stem cell behaviour and phenotype. *Biomaterials* **32**, 5979–5993 (2011).

12. O. Chaudhuri, J. Cooper-White, P. A. Janmey, D. J. Mooney, V. B. Shenoy, Effects of extracellular matrix viscoelasticity on cellular behaviour. *Nature* **584**, 535–546 (2020).

13. O. Chaudhuri, L. Gu, M. Darnell, D. Klumpers, S. A. Bencherif, J. C. Weaver, N. Huebsch, D. J. Mooney, Substrate stress relaxation regulates cell spreading. *Nat. Commun.* **6**, 6364 (2015).

14. I. A. Marozas, K. S. Anseth, J. J. Cooper-White, Adaptable boronate ester hydrogels with tunable viscoelastic spectra to probe timescale dependent mechanotransduction. *Biomaterials* **223**, 119430 (2019).

15. A. Bauer, L. Gu, B. Kwee, W. A. Li, M. Dellacherie, A. D. Celiz, D. J. Mooney, Hydrogel substrate stress-relaxation regulates the spreading and proliferation of mouse myoblasts. *Acta Biomater.* **62**, 82–90 (2017).

16. S. M. Lien, L. Y. Ko, T. J. Huang, Effect of pore size on ECM secretion and cell growth in gelatin scaffold for articular cartilage tissue engineering. *Acta Biomater.* **5**, 670–679 (2009).

17. E. E. Charrier, K. Pogoda, R. G. Wells, P. A. Janmey, Control of cell morphology and differentiation by substrates with independently tunable elasticity and viscous dissipation. *Nat. Commun.* **9**, 449 (2018).

18. C. E. Chan, D. J. Odde, Traction dynamics of filopodia on compliant substrates. *Science* **322**, 1687–1691 (2008).

19. H. Baumann, M. Schwingel, M. Sestu, A. Burcza, S. Marg, W. Ziegler, A. V. Taubenberger, D. J. Muller, M. Bastmeyer, C. M. Franz, Biphasic reinforcement of nascent adhesions by vinculin. *J. Mol. Recognit.* **36**, e3012 (2023).

20. Z. Gong, S. E. Szczesny, S. R. Caliari, E. E. Charrier, O. Chaudhuri, X. Cao, Y. Lin, R. L. Mauck, P. A. Janmey, J. A. Burdick, V. B. Shenoy, Matching material and cellular timescales maximizes cell spreading on viscoelastic substrates. *Proc. Natl. Acad. Sci. U.S.A.* **115**, E2686–E2695 (2018).

21. B. Cheng, M. Li, W. Wan, H. Guo, G. M. Genin, M. Lin, F. Xu, Predicting YAP/TAZ nuclear translocation in response to ECM mechanosensing. *Biophys. J.* **122**, 43–53 (2023).

22. S. Lv, D. M. Dudek, Y. Cao, M. M. Balamurali, J. Gosline, H. Li, Designed biomaterials to mimic the mechanical properties of muscles. *Nature* **465**, 69–73 (2010).

23. C. Huerta-Lopez, J. Alegre-Cebollada, Protein hydrogels: The Swiss army knife for enhanced mechanical and bioactive properties of biomaterials. *Nanomaterials* **11**, 1656 (2021).

24. J. Alegre-Cebollada, Protein nanomechanics in biological context. *Biophys. Rev.* **13**, 435–454 (2021).

25. F. Saqlain, I. Popa, J. M. Fernandez, J. Alegre-Cebollada, A novel strategy for utilizing voice coil servoactuators in tensile tests of low volume protein hydrogels. *Macromol. Mater. Eng.* **300**, 369–376 (2015).

26. M. Carrion-Vazquez, H. Li, H. Lu, P. E. Marszalek, A. F. Oberhauser, J. M. Fernandez, The mechanical stability of ubiquitin is linkage dependent. *Nat. Struct. Biol.* **10**, 738–743 (2003).

27. D. J. Brockwell, E. Paci, R. C. Zinober, G. S. Beddard, P. D. Olmsted, D. A. Smith, R. N. Perham, S. E. Radford, Pulling geometry defines the mechanical resistance of a β-sheet protein. *Nat. Struct. Mol. Biol.* **10**, 731–737 (2003).

28. J. Oroz, M. Bruix, D. V. Laurents, A. Galera-Prat, J. Schonfelder, F. J. Canada, M. Carrion-Vazquez, The Y9P variant of the titin I27 module: Structural determinants of its revisited nanomechanics. *Structure* **24**, 606–616 (2016).

29. Á. Pérez-Benito, C. Huerta-López, J. Alegre-Cebollada, J. M. García-Aznar, S. Hervas-Raluy, Computational modelling of the mechanical behaviour of protein-based hydrogels. *J. Mech. Behav. Biomed. Mater.* **138**, 105661 (2023).

30. K. C. Wang, Y. T. Yeh, P. Nguyen, E. Limqueco, J. Lopez, S. Thorossian, K. L. Guan, Y. J. Li, S. Chien, Flow-dependent YAP/TAZ activities regulate endothelial phenotypes and atherosclerosis. *Proc. Natl. Acad. Sci. U.S.A.* **113**, 11525–11530 (2016).

31. S. L. Bellis, Advantages of RGD peptides for directing cell association with biomaterials. *Biomaterials* **32**, 4205–4210 (2011).

32. W. R. Legant, J. S. Miller, B. L. Blakely, D. M. Cohen, G. M. Genin, C. S. Chen, Measurement of mechanical tractions exerted by cells in three-dimensional matrices. *Nat. Methods* **7**, 969–971 (2010).

33. I. Andreu, B. Falcones, S. Hurst, N. Chahare, X. Quiroga, A. L. Le Roux, Z. Kechagia, A. E. M. Beedle, A. Elosegui-Artola, X. Trepat, R. Farre, T. Betz, I. Almendros, P. Roca-Cusachs, The force loading rate drives cell mechanosensing through both reinforcement and cytoskeletal softening. *Nat. Commun.* **12**, 4229 (2021).

34. M. A. Rahman, M. Ušaj, D. E. Rassier, A. Månsson, Blebbistatin effects expose hidden secrets in the force-generating cycle of actin and myosin. *Biophys. J.* **115**, 386–397 (2018).

35. C. Venturini, P. Sáez, A multi-scale clutch model for adhesion complex mechanics. *PLoS Comput. Biol.* **19**, e1011250 (2023).

36. R. Tapia-Rojo, A. Alonso-Caballero, J. M. Fernandez, Direct observation of a coil-to-helix contraction triggered by vinculin binding to talin. *Sci. Adv.* **6**, eaaz4707 (2020).

37. S. J. Han, E. V. Azarova, A. J. Whitewood, A. Bachir, E. Guttierrez, A. Groisman, A. R. Horwitz, B. T. Goult, K. M. Dean, G. Danuser, Pre-complexation of talin and vinculin without tension is required for efficient nascent adhesion maturation. *eLife* **10**, e66151 (2021).

38. K. Austen, P. Ringer, A. Mehlich, A. Chrostek-Grashoff, C. Kluger, C. Klingner, B. Sabass, R. Zent, M. Rief, C. Grashoff, Extracellular rigidity sensing by talin isoform-specific mechanical linkages. *Nat. Cell Biol.* **17**, 1597–1606 (2015).

39. T. N. Wight, M. J. Merrilees, Proteoglycans in atherosclerosis and restenosis. *Circ. Res.* **94**, 1158–1167 (2004).

40. B. Duran-Jimenez, D. Dobler, S. Moffatt, N. Rabbani, C. H. Streuli, P. J. Thornalley, D. R. Tomlinson, N. J. Gardiner, Advanced glycation end products in extracellular matrix proteins contribute to the failure of sensory nerve regeneration in diabetes. *Diabetes* **58**, 2893–2903 (2009).

41. N. G. Frangogiannis, The extracellular matrix in myocardial injury, repair, and remodeling. *J. Clin. Invest.* **127**, 1600–1612 (2017).

42. N. R. Peter, G. Maurice, The molecular genetics of Marfan syndrome and related microfibrillopathies. *J. Med. Genet.* **37**, 9 (2000).

43. J. Huang, L. Zhang, D. Wan, L. Zhou, S. Zheng, S. Lin, Y. Qiao, Extracellular matrix and its therapeutic potential for cancer treatment. *Signal Transduct. Target. Ther.* **6**, 153 (2021).

44. B. S. Brooke, J. P. Habashi, D. P. Judge, N. Patel, B. Loeys, H. C. Dietz, Angiotensin II blockade and aortic-root dilation in Marfan's syndrome. *N. Engl. J. Med.* **358**, 2787–2795 (2008).

45. J. Bonafont, Á. Mencía, M. García, R. Torres, S. Rodríguez, M. Carretero, E. Chacón-Solano, S. Modamio-Høybjør, L. Marinas, C. León, M. J. Escamez, I. Hausser, M. Del Río, R. Murillas, F. Larcher, Clinically relevant correction of recessive dystrophic epidermolysis bullosa by dual sgRNA CRISPR/Cas9-mediated gene editing. *Mol. Ther.* **27**, 986–998 (2019).

46. B. L. LeSavage, D. Zhang, C. Huerta-López, A. E. Gilchrist, B. A. Krajina, K. Karlsson, A. R. Smith, K. Karagyozova, K. C. Klett, M. S. Huang, C. Long, G. Kaber, C. M. Madl, P. L. Bollyky, C. Curtis, C. J. Kuo, S. C. Heilshorn, Engineered matrices reveal stiffness-mediated chemoresistance in patient-derived pancreatic cancer organoids. *Nat. Mater.* **23**, 1138–1149 (2024).

47. E. Hui, K. I. Gimeno, G. Guan, S. R. Caliari, Spatiotemporal control of viscoelasticity in phototunable hyaluronic acid hydrogels. *Biomacromolecules* **20**, 4126–4134 (2019).

48. V. Panzetta, S. Fusco, P. A. Netti, Cell mechanosensing is regulated by substrate strain energy rather than stiffness. *Proc. Natl. Acad. Sci. U.S.A.* **116**, 22004–22013 (2019).

49. K. M. Wisdom, K. Adebowale, J. Chang, J. Y. Lee, S. Nam, R. Desai, N. S. Rossen, M. Rafat, R. B. West, L. Hodgson, O. Chaudhuri, Matrix mechanical plasticity regulates cancer cell migration through confining microenvironments. *Nat. Commun.* **9**, 4144 (2018).

50. K. Adu-Berchie, Y. Liu, D. K. Y. Zhang, B. R. Freedman, J. M. Brockman, K. H. Vining, B. A. Nerger, A. Garmilla, D. J. Mooney, Generation of functionally distinct T-cell populations by altering the viscoelasticity of their extracellular matrix. *Nat. Biomed. Eng.* **7**, 1374–1391 (2023).

51. J. Li, D. J. Mooney, Designing hydrogels for controlled drug delivery. *Nat. Rev. Mater.* **1**, 16071 (2016).

52. D. H. Kim, M. Abidian, D. C. Martin, Conducting polymers grown in hydrogel scaffolds coated on neural prosthetic devices. *J. Biomed. Mater. Res. A* **71**, 577–585 (2004).

53. S. Zhang, A. M. Bellinger, D. L. Glettig, R. Barman, Y.-A. L. Lee, J. Zhu, C. Cleveland, V. A. Montgomery, L. Gu, L. D. Nash, D. J. Maitland, R. Langer, G. Traverso, A pH-responsive supramolecular polymer gel as an enteric elastomer for use in gastric devices. *Nat. Mater.* **14**, 1065–1071 (2015).

54. J. Liu, Y. Pang, S. Zhang, C. Cleveland, X. Yin, L. Booth, J. Lin, Y.-A. Lucy Lee, H. Mazdiyasni, S. Saxton, A. R. Kirtane, T. von Erlach, J. Rogner, R. Langer, G. Traverso, Triggerable tough hydrogels for gastric resident dosage forms. *Nat. Commun.* **8**, 124 (2017).

55. M. Vicente-Manzanares, X. Ma, R. S. Adelstein, A. R. Horwitz, Non-muscle myosin II takes centre stage in cell adhesion and migration. *Nat. Rev. Mol. Cell. Biol.* **10**, 778–790 (2009).

56. K. Mandal, Z. Gong, A. Rylander, V. B. Shenoy, P. A. Janmey, Opposite responses of normal hepatocytes and hepatocellular carcinoma cells to substrate viscoelasticity. *Biomater. Sci.* **8**, 1316–1328 (2020).

57. T. Iskratsch, H. Wolfenson, M. P. Sheetz, Appreciating force and shape—The rise of mechanotransduction in cell biology. *Nat. Rev. Mol. Cell. Biol.* **15**, 825–833 (2014).

58. B. Geiger, K. M. Yamada, Molecular architecture and function of matrix adhesions. *Cold Spring Harb. Perspect. Biol.* **3**, a005033 (2011).

59. B. Klapholz, N. H. Brown, Talin—The master of integrin adhesions. *J. Cell Sci.* **130**, 2435–2446 (2017).

60. B. T. Goult, J. Yan, M. A. Schwartz, Talin as a mechanosensitive signaling hub. *J. Cell Biol.* **217**, 3776–3784 (2018).

61. R. Tapia-Rojo, M. Mora, S. Board, J. Walker, R. Boujemaa-Paterski, O. Medalia, S. Garcia-Manyes, Enhanced statistical sampling reveals microscopic complexity in the talin mechanosensor folding energy landscape. *Nat. Phys.* **19**, 52–60 (2023).

62. M. A. Bodescu, J. Aretz, M. Grison, M. Rief, R. Fässler, Kindlin stabilizes the talin·integrin bond under mechanical load by generating an ideal bond. *Proc. Natl. Acad. Sci. U.S.A.* **120**, e2218116120 (2023).

63. B. Chen, B. Ji, H. Gao, Modeling active mechanosensing in cell–matrix interactions. *Annu. Rev. Biophys.* **44**, 1–32 (2015).

64. A. B. Kobb, T. Zulueta-Coarasa, R. Fernandez-Gonzalez, Tension regulates myosin dynamics during Drosophila embryonic wound repair. *J. Cell. Sci.* **130**, 689–696 (2017).

65. M. Kovács, K. Thirumurugan, P. J. Knight, J. R. Sellers, Load-dependent mechanism of nonmuscle myosin 2. *Proc. Natl. Acad. Sci. U.S.A.* **104**, 9994–9999 (2007).

66. A. Nabavizadeh, M. Bayat, V. Kumar, A. Gregory, J. Webb, A. Alizad, M. Fatemi, Viscoelastic biomarker for differentiation of benign and malignant breast lesion in ultra- low frequency range. *Sci. Rep.* **9**, 5737 (2019).

67. F. Zanconato, M. Cordenonsi, S. Piccolo, YAP/TAZ at the roots of cancer. *Cancer Cell* **29**, 783–803 (2016).

68. H. L. Sladitschek-Martens, A. Guarnieri, G. Brumana, F. Zanconato, G. Battilana, R. L. Xiccato, T. Panciera, M. Forcato, S. Bicciato, V. Guzzardo, M. Fassan, L. Ulliana, A. Gandin, C. Tripodo, M. Foiani, G. Brusatin, M. Cordenonsi, S. Piccolo, YAP/TAZ activity in stromal cells prevents ageing by controlling cGAS-STING. *Nature*, **607**, 790–798 (2022).

69. T. Sadhanasatish, K. Augustin, L. Windgasse, A. Chrostek-Grashoff, M. Rief, C. Grashoff, A molecular optomechanics approach reveals functional relevance of force transduction across talin and desmoplakin. *Sci. Adv.* **9**, eadg3347 (2023).

70. D. A. Fancy, T. Kodadek, Chemistry for the analysis of protein-protein interactions: Rapid and efficient cross-linking triggered by long wavelength light. *Proc. Natl. Acad. Sci. U.S.A.* **96**, 6020–6024 (1999).

71. R. Garcia, Nanomechanical mapping of soft materials with the atomic force microscope: Methods, theory and applications. *Chem. Soc. Rev.* **49**, 5850–5884 (2020).

72. R. Madurga, A. M. Ganan-Calvo, G. R. Plaza, G. V. Guinea, M. Elices, J. Perez-Rigueiro, Production of high performance bioinspired silk fibers by straining flow spinning. *Biomacromolecules* **18**, 1127–1133 (2017).

73. R. S. Fischer, K. A. Myers, M. L. Gardel, C. M. Waterman, Stiffness-controlled three-dimensional extracellular matrices for high-resolution imaging of cell behavior. *Nat. Protoc.* **7**, 2056–2066 (2012).

74. K. Kartasalo, R.-P. Pölönen, M. Ojala, J. Rasku, J. Lekkala, K. Aalto-Setälä, P. Kallio, CytoSpectre: A tool for spectral analysis of oriented structures on cellular and subcellular levels. *BMC Bioinformatics* **16**, 344 (2015).

75. D. Roylance. Engineering Viscoelasticity. (2001); https://ocw.mit.edu/courses/3-11-mechanics-of-materials-fall-1999/resources/mit3_11f99_visco/.

76. G. I. Bell, Models for the specific adhesion of cells to cells. *Science* **200**, 618–627 (1978).

77. S. Improta, A. S. Politou, A. Pastore, Immunoglobulin-like modules from titin I-band: Extensible components of muscle elasticity. *Structure* **4**, 323–337 (1996).

78. K. Yagawa, K. Yamano, T. Oguro, M. Maeda, T. Sato, T. Momose, S. Kawano, T. Endo, Structural basis for unfolding pathway-dependent stability of proteins: Vectorial unfolding versus global unfolding. *Protein. Sci.* **19**, 693–702 (2010).

79. J. Fang, A. Mehlich, N. Koga, J. Huang, R. Koga, X. Gao, C. Hu, C. Jin, M. Rief, J. Kast, D. Baker, H. Li, Forced protein unfolding leads to highly elastic and tough protein hydrogels. *Nat. Commun.* **4**, 2974 (2013).

80. E. Gasteiger, C. Hoogland, A. Gattiker, S. Duvaud, M. R. Wilkins, R. D. Appel, A. Bairoch, *The Proteomics Protocols Handbook*, J. M. Walker, Ed. (Humana Press, 2005), pp. 571–607.